

Contents lists available at [ScienceDirect](https://www.sciencedirect.com)

Developmental Biology

journal homepage: www.elsevier.com/locate/developmentalbiology

Original research article

Pronounced early differentiation underlies zebra finch gonadal germ cell development

Matthew T. Biegler^{a,*,**}, Kirubel Belay^a, Wei Wang^a, Christina Szialta^a, Paul Collier^b, Ji-Dung Luo^a, Bettina Haase^a, Gregory L. Gedman^a, Asha V. Sidhu^a, Elijah Harter^a, Carlos Rivera-López^c, Kwame Amoako-Boadu^d, Olivier Fedrigo^a, Hagen U. Tilgner^b, Thomas Carroll^a, Erich D. Jarvis^{a,e,*}, Anna L. Keyte^{a,***}

^a The Rockefeller University, New York NY, USA^b Weill Cornell Medicine, New York NY, USA^c Harvard University, Cambridge, MA, USA^d New York University, New York NY, USA^e Howard Hughes Medical Institute, Chevy Chase, MD, USA

A B S T R A C T

The diversity of germ cell developmental strategies has been well documented across many vertebrate clades. However, much of our understanding of avian primordial germ cell (PGC) specification and differentiation has derived from only one species, the chicken (*Gallus gallus*). Of the three major classes of birds, chickens belong to Galloanserae, representing less than 4% of species, while nearly 95% of extant bird species belong to Neoaves. This represents a significant gap in our knowledge of germ cell development across avian species, hampering efforts to adapt genome editing and reproductive technologies developed in chicken to other birds. We therefore applied single-cell RNA sequencing to investigate inter-species differences in germ cell development between chicken and zebra finch (*Taeniopygia castanotis*), a Neoaves songbird species and a common model of vocal learning. Analysis of early embryonic male and female gonads revealed the presence of two distinct early germ cell types in zebra finch and only one in chicken. Both germ cell types expressed zebra finch Germline Restricted Chromosome (GRC) genes, present only in songbirds among birds. One of the zebra finch germ cell types expressed the canonical PGC markers, as did chicken, but with expression differences in several signaling pathways and biological processes. The second zebra finch germ cell cluster was marked by proliferation and fate determination markers, indicating beginning of differentiation. Notably, these two zebra finch germ cell populations were present in both male and female zebra finch gonads as early as HH25. Using additional chicken developmental stages, similar germ cell heterogeneity was identified in the more developed gonads of females, but not males. Overall, our study demonstrates a substantial heterochrony in zebra finch germ cell development compared to chicken, indicating a richer diversity of avian germ cell developmental strategies than previously known.

1. Introduction

Birds have been foundational model organisms in disciplines as varied as ecology, evolutionary biology, developmental biology and neuroscience. However, compared to other groups of model organisms, the development of genetically modified avian models, including transgenic animal lines, has been quite limited. Genome editing has been most successful in the chicken (*Gallus gallus*), particularly through germline transmission using cultured primordial germ cells (PGCs) (Ballantyne et al., 2021b; Choi et al., 2010; Kim et al., 2010; van de Lavoie et al., 2006; Lyall et al., 2011; Motono et al., 2008). PGCs are

early germline stem cells that give rise to egg and sperm cells. During embryonic development in birds and some reptiles, PGCs migrate from the germinal crescent to the gonadal ridges via the vascular system (Fujimoto et al., 1979; Swift, 1914). Upon reaching the developing gonad, PGCs undergo clonal expansion and apoptotic pruning before entering a quiescent state in embryonic males or committing to a meiotic fate in embryonic females (Ballantyne et al., 2021a; Cantú and Laird, 2017; Ichikawa and Horiuchi, 2023). Genome editing methods in chicken take advantage of this developmental process by harvesting PGCs from embryonic blood at Hamburger-Hamilton (HH) stage 13–16 or embryonic gonads at HH28, genetically manipulating them *in vitro*,

* Corresponding author. The Rockefeller University, New York NY, USA.

** Corresponding author.

*** Corresponding author.

E-mail addresses: mbiegler@rockefeller.edu (M.T. Biegler), ejarvis@rockefeller.edu (E.D. Jarvis), anna@colossal.com (A.L. Keyte).<https://doi.org/10.1016/j.ydbio.2024.08.006>

Received 29 April 2024; Received in revised form 22 July 2024; Accepted 14 August 2024

Available online 28 August 2024

0012-1606/© 2024 The Authors. Published by Elsevier Inc. This is an open access article under the CC BY license (<http://creativecommons.org/licenses/by/4.0/>).

and reintroducing them into the bloodstream of host embryos when PGC migration occurs. This allows manipulated cells to colonize the gonads as they would during normal development and subsequently contribute to the next generation.

Despite the successes in chicken, PGC-mediated genome editing and germline transmission have been difficult to apply in other bird species. Chicken is the only species for which PGCs have successfully been cultured for extended periods and maintained their commitment to the germ line (van de Lavoie et al., 2006). Short-term (2–6 passages) PGC cultures have been performed for several non-chicken species, including Japanese quail (*Coturnix japonica*), duck (*Anas platyrhynchos*), and zebra finch (*Taeniopygia castanotis*, formerly *Taeniopygia guttata castanotis*) (Chen et al., 2019; Gessara et al., 2021; Imus et al., 2014; Jung et al., 2019; Park et al., 2008; Wernery et al., 2010; Yakhkeshi et al., 2017), but long-term culture methods have not been reported. Chicken is a Galloanserae bird, which diverged over 90 million years ago with Neoaves species; in comparison most Neoaves orders diverged between 65 and 50 million years ago (Jarvis et al., 2014). Neoaves make up 95% of the more than 10,000 living bird species. Therefore, studies of germ cell development and subsequent establishment of a Neoaves PGC culture system is more likely to be applicable to birds generally.

An additional consideration in choosing a species to capture the diversity of avian development is the presence of the germline-restricted chromosome (GRC) in songbirds (Oscine Passeriformes). Songbirds, which include the zebra finch, constitute approximately 5,000, or half of all bird species (Ericson et al., 2003). The songbird GRC is found only in germ cells, as it is eliminated from somatic cells during embryonic development (Pigozzi and Solari, 1998; Torgasheva et al., 2019). GRC genes appear to have originated from regional duplication events of the autosomes and sex chromosomes (A chromosomes), without loss of the original genes (Borodin et al., 2022). Songbird GRC genes have only begun to be identified, as the chromosome is challenging to assemble due to the high number of highly conserved and repetitive sequences (Biederman et al., 2018; Kinsella et al., 2019). From sequencing that has been completed, it is known that the genes on the zebra finch GRC are expressed in adult testes and ovaries, and many identified genes are involved in female gonad development (Kinsella et al., 2019).

In our study, we sought to identify potential molecular differences that could explain the efficacy in *in vitro* culture conditions between chicken and zebra finch gonadal PGCs, using scRNAseq data, and compared our findings to two recent reports conducted independently (Jung et al., 2021, 2023). We found that by HH28 of both sexes, there exist two populations of zebra finch germ cells (not three as found in Jung et al., 2021), but only one at the same stage in chicken. A parallel second cluster appeared in chicken by HH36, but only in females. These two populations in zebra finch differ in expression of key transcription factors and signaling pathways that play distinct roles in germ cell biology and differentiation, as well as differential expression of GRC genes.

2. Results

2.1. Zebra finch gonadal scRNAseq identifies two germ cell populations

Male (n = 2) and female (n = 2) zebra finch gonads were dissected and dissociated at HH28 (around 5.5 days of development; Murray et al., 2013), a stage at which avian gonadal PGCs have previously been collected for cell culture (Choi et al., 2010; Jung et al., 2019) (Fig. S1A; Table S1). Samples were processed for scRNAseq using the 10x Genomics platform, and the reads mapped against a high-quality zebra finch reference assembly (21,762 gene annotations; Table S2) produced by the Vertebrate Genomes Project (GCF_003957565.221; Rhie et al., 2021). Embryo sex was validated by W chromosome gene expression (Fig. S1B). This mapping and a stringent quality control pipeline were used to remove confounding artifacts commonly seen in scRNAseq analysis (Luecken and Theis, 2019) (Figs. S1C–S1G; Table S3). A total of 8970

cells passed quality control.

Gene expression-based PCA analyses were visualized by UMAP dimensional reduction, with 26 nearest-neighbor clusters resolved (Fig. 1A). To identify cell types among these clusters, we assign labels to a strict subset of cells marked by canonical cell type gene expression patterns (Fig. S2A; Table S4). The gene expression profiles of these assigned cell types were then applied as a reference in a label transfer analysis (Stuart et al., 2019), inferring the cell types of the remaining cells by gene expression profile similarity (Figs. S2B–S2D). Both male and female populations included the expected major gonadal cell types (Fig. 1B) seen in other species at this stage of development (Estermann et al., 2020b; Jung et al., 2021; Stévant et al., 2019) (Fig. S2B). By combining the cell-type labels with clusters, we identified several cell subtypes, including two groups of epithelial cells, three groups of interstitial cells, and two groups of putative intermediate mesodermal (IM) progenitor populations (Fig. 1C).

Two distinct but hierarchically-related clusters, c18 and c11, were identified as expressing the germ cell markers *DAZL*, *DDX4* and *DND1* (Fig. 1B–C and S2A–B), which we broadly defined as zebra finch germ cell clusters 1 and 2 (zGC1 and zGC2). These two clusters were stably resolved across UMAs generated with varying numbers of dimensions (Fig. S1H) and nearest-neighbor clustering resolutions (Fig. S1I). Both zGC clusters contained cells from males and females (Fig. S2C), indicating that clustering was not due to sex. Both clusters were also marked by increased unique molecular index (UMI) read counts and gene counts (Fig. S2D), consistent with recent findings of stem cell hypertranscription (Kim et al., 2023). Interestingly, only zGC1 expressed *NANOG* (Fig. 1D), a canonical marker of embryonic stem cells and PGCs (Chambers et al., 2007; Jean et al., 2015).

2.2. The two zebra finch germ cell populations dynamically express GRC genes

We next wanted to determine the extent of gene expression in the two zGC clusters from the GRC, which is obligately present in the germline of all passerines (Pigozzi and Solari, 1998; Torgasheva et al., 2019). However, as the zebra finch GRC has not yet been sequenced in its entirety and no gene annotations exist in the current reference genome (GCF_003957565.2), we hypothesized that GRC gene transcripts in the zebra finch germ cells may be mapping to conserved paralog annotations on the A chromosomes (Fig. 2A). Of the high-confidence GRC candidate gene paralogs identified in the A chromosomes of a previous reference genome version (GCF_000151805.1; Kinsella et al., 2019), we identified 77 in the current reference assembly used to analyze our scRNAseq datasets (Table S5). Compared to somatic cell types in the gonad, 24 of these candidate genes were upregulated in at least one of the zGC clusters (Fig. 2B and S3; Table S6). These included genes related to TGF- β superfamily/SMAD signaling pathways (*BMPRI1B*), RA response-mediated gene expression (*RXRA*), and canonical PGC identity (*PRDM1*, also known as *BLIMP-1*). Additionally, 13 GRC candidate genes were differentially expressed between the two zGC populations (\log_2 fold-change ≥ 0.5 and adjusted p-value ≤ 0.05). Using an aggregate geneset of GRC gene candidates for UCell module analysis (Andreatta and Carmona, 2021), we saw significantly higher module scores in both zGC populations compared to somatic cell types (Fig. 2C; Table S7), indicating that significant GRC gene expression was indeed being incorrectly captured as A chromosome gene expression.

To further resolve the potential involvement of the GRC in zebra finch germ cell heterogeneity, four published sequences of GRC genes were appended to our scRNAseq dataset: *NAPA_{GRC}*, *TRIM71_{GRC}*, *ELAVL4_{GRC}* and *BICC1_{GRC}* (Biederman et al., 2018; Kinsella et al., 2019). We quantified the extent to which the GRC gene copies map uniquely to the GRC versus the corresponding A chromosome paralogs, mapping simulated reads for each gene onto a small, simulated genome containing the eight gene annotations. We found that, on average, more than 90% of reads mapped uniquely to their respective chromosomal

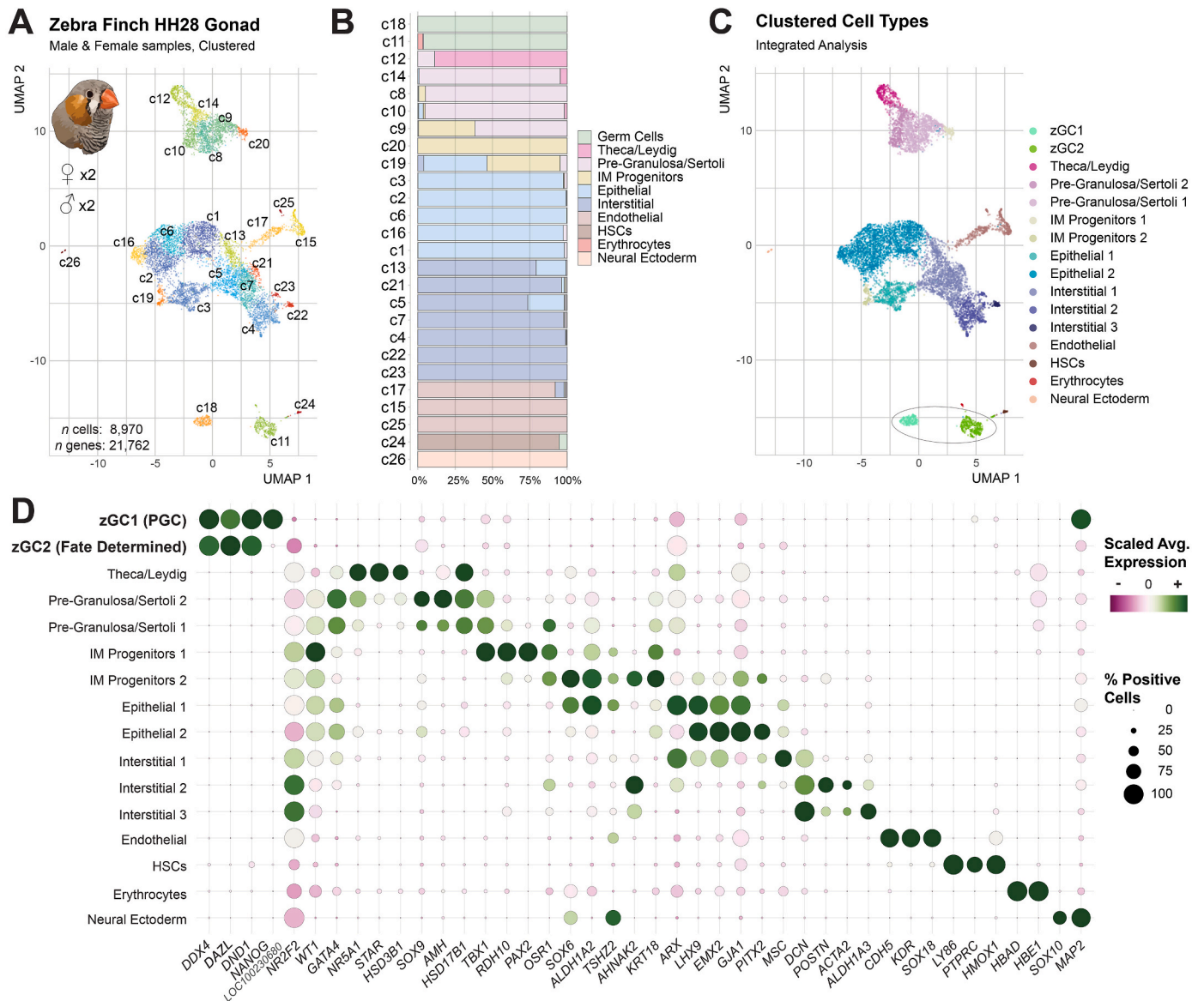


Fig. 1. Identification of two germ cell types in the zebra finch gonad. **A.** UMAP plot of male and female zebra finch gonadal nearest-neighbor cell clusters at HH28. Further information on quality control and dimensional reduction for this dataset may be found in [Figure S1](#). **B.** Proportional bar chart of inferred cell types present in each nearest-neighbor cluster. **C.** UMAP plot of male and female zebra finch clustered cell types at HH28. See [Fig. S2](#) for more information on designation. **D.** Dot plot of scaled expression for select gene markers of each clustered cell type.

gene origin ([Fig. 2D](#)), particularly for *TRIM71*, *NAPA*, and *ELAVL4*. This simulation demonstrated that scRNAseq reads from the closely related GRC and A chromosome paralogs can be confidently distinguished and mapped.

Mapping GRC gene expression onto the UMAP cell cluster diagram allowed us to independently verify the exclusion of the GRC from all other gonadal cell types, as expression of *NAPAGRC*, *TRIM71GRC*, *ELAVL4GRC* and *BICC1GRC* was primarily restricted to the two germ cell clusters ([Fig. S3](#), red-labeled genes). For example, *NAPAGRC* was expressed in 83% of zGC1 and 100% of zGC2 cells, and only 0.5% of cells in somatic clusters ([Table S6](#)). Altogether, we detected GRC gene expression in 535 of 542 germ cell barcodes. *TRIM71GRC* and *BICC1GRC* expression was weak compared to their respective A chromosome paralogs ([Figs. S4A–S4B](#)), while *ELAVL4GRC* and *NAPAGRC* were expressed at higher levels in the germ cells than *ELAVL4A* (Chr. 8) and *NAPAA* (Chr. 34). These GRC paralogs were particularly upregulated in the zGC2 cluster ([Fig. 2E–F](#)), indicating differential gene expression between germ cell types.

We generated *in situ* hybridization probes for a minimally conserved (81.7% identity) region of the ChrA and GRC *NAPA* paralogs, which demonstrated differential signals in the zebra finch embryonic gonad ([Figs. S5A–S5C](#)), namely the specificity of the *NAPAGRC* probe to gonadal cells. Using probes for *DND1* and *DAZL* germ cell markers (selected for high and consistent expression across zGC clusters; [Fig. S5D](#)), we validated *NAPAGRC* expression by dual-label fluorescent *in situ* hybridization ([Fig. 2G](#) and [S5E](#)), which showed robust expression in a subset of germ cells in both female and male gonads. Further analysis showed that high-expression *NAPAGRC* germ cells poorly co-localized with *NANOG* ([Fig. 2H](#)), consistent with the lower expression of *NAPAGRC* in the zGC1 cluster from the scRNAseq analyses. These findings indicate that the two zebra finch germ cells clusters clearly and differentially express GRC gene paralogs during early gonadal development.

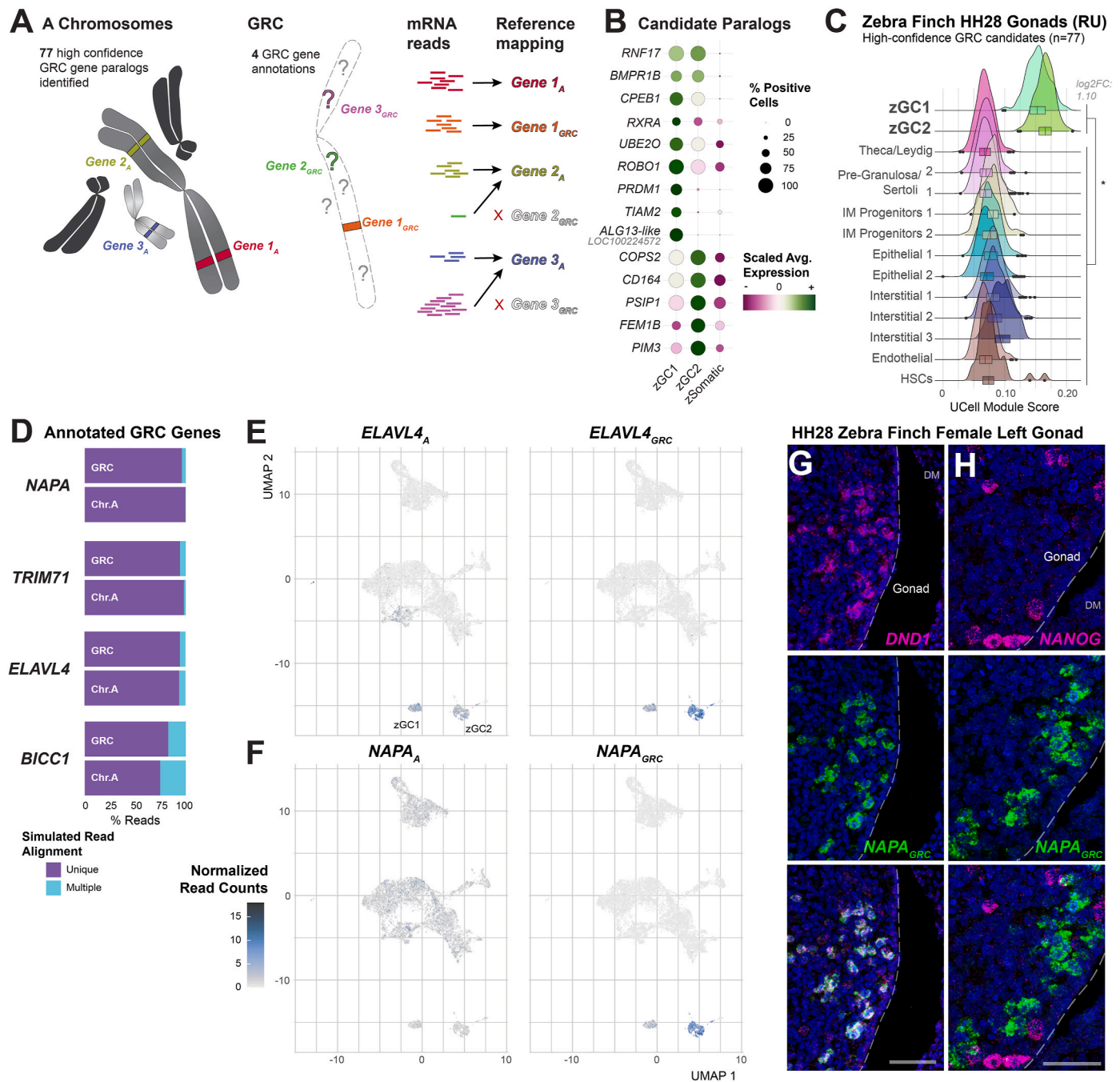


Fig. 2. Assessment of germline-restricted chromosome genes in the zebra finch HH28 gonad. **A.** Diagram of putative GRC gene read mapping onto annotated somatic gene paralogs. 81 GRC candidates were identified in the current annotation used in this study, 4 of which possess available sequences for germ cell deconvolution. **B.** Scaled-expression dot plot of select 15 high-confidence GRC gene candidates (Kinsella et al., 2019) between zGC1, zGC2, and somatic cells. **C.** Module score assessment of the 77 unmapped, high-confidence GRC gene candidates in each clustered cell type. A $\text{Log}_2\text{FC} > 0.5$ between zGC and zSomatic populations and a $p\text{-value} \leq 0.05$ by two-sided t -test (Table S33) is denoted by *. Heatmap of expression for individual genes may be found in Figure S3. **D.** Simulated read multi-mapping assessment between GRC and A chromosome gene pairs. **E.** UMAP plots of zebra finch male and female HH28 zebra finch gonads overlaid with *ELAVL4_A* (left) and *ELAVL4_{GRC}* (right) gene pair expression (transcripts/10,000 UMIs) for all cell barcodes. Note the high specificity of the GRC paralog sequences with the zGC clusters, particularly in zGC2. **F.** UMAP plots of zebra finch male and female HH28 zebra finch gonads overlaid with *NAPA_A* (left) and *NAPA_{GRC}* (right) gene pair expression (transcripts/10,000 UMIs) for all cell barcodes. Note the high specificity of the GRC paralog sequences with the zGC clusters, particularly in zGC2. **G.** Dual-labeled fluorescent *in situ* hybridization of *DND1* and *NAPA_{GRC}* in the HH28 zebra finch, showing high co-localization near the medial edge of the female left gonad. Arrows highlight *DND1*+ cells with low *NAPA_{GRC}* expression. Scale bar = 50 μm . **H.** Dual-labeled fluorescent *in situ* hybridization of *NANOG* and *NAPA_{GRC}* in the HH28 zebra finch female left gonad, showing very little co-localization. Scale bar = 50 μm .

2.3. The two zebra finch gonadal germ cell clusters represent developmentally distinct states

To further determine how the zGC1 and zGC2 clusters differ from

somatic cells, we assessed differentially expressed genes (DEGs) between the transcriptomes of the zGC clusters and the somatic (zSomatic) gonadal cells, with DEGs defined as genes with expression in $\geq 10\%$ of cells in the target cluster, a log-fold change ≥ 0.5 and an adjusted p -value

<0.05. Both zGC1 and zGC2 shared 1077 DEGs relative to zSomatic clusters (524-up and 553-down regulated; Fig. 3A; Table S6); these included other general germ cell markers not noted above, such as *TDRD15*, *PIWIL1*, *MAEL* and *SMC1B* (Fig. 3B). Another 1093 DEGs were identified only for zGC1; these included several canonical PGC pluripotency markers, such as *PRDM14* and *KIT* (Fig. 3B) (Magnúsdóttir et al., 2013; Srihawong et al., 2016). Notably, these canonical PGC markers were largely absent or lowly expressed in zGC2.

We identified 648 DEGs between zGC2 and zSomatic clusters; these included several homeobox (e.g., *YBX1*, *GBX2*, *DLX2*) and POU domain (e.g., *POU3F2*, *POU3F4*) transcription factors (Fig. 3B). zGC2 also showed strong upregulation of fate determination markers *MEIOC*, *REC8* (*LOC121468792*), and *FOXL2L* (*LOC101233936*). *FOXL2L* (alternatively *FOXL3-like*) is a gene lost in placental mammals (Bertho et al., 2016) that

has been identified as a cell-intrinsic suppressor of spermatogenesis in medaka fish (Nishimura et al., 2015) and a driver of oogonial progenitor cell fate determination in zebrafish (Liu et al., 2022). In these models *FOXL2L* expression also coincided with increased cell proliferation, and we noted that many zGC2 DEGs were gene markers of cell proliferation relating to the mitotic cell cycle (*MKI67*, *CDCA3*, *PCNA*, *CEP55*) and oxidative phosphorylation pathways (*HMGB1*, *CHCHD2*) (Aras et al., 2015; Tang et al., 2011; Yao et al., 2019). Indeed, cell cycle scoring indicated that 55% of zGC2 cells were in the G2 or M phase compared to 22% of zGC1 cells (Fig. S2D; Table S3). This difference persisted despite cell cycle regression during the clustering workflow.

Focusing on the zGC clusters, we visually confirmed significant representation of zGC clusters in the male and female datasets (Fig. 3C). Between zGC1 and zGC2 we identified 956 DEGs, with the most distinct

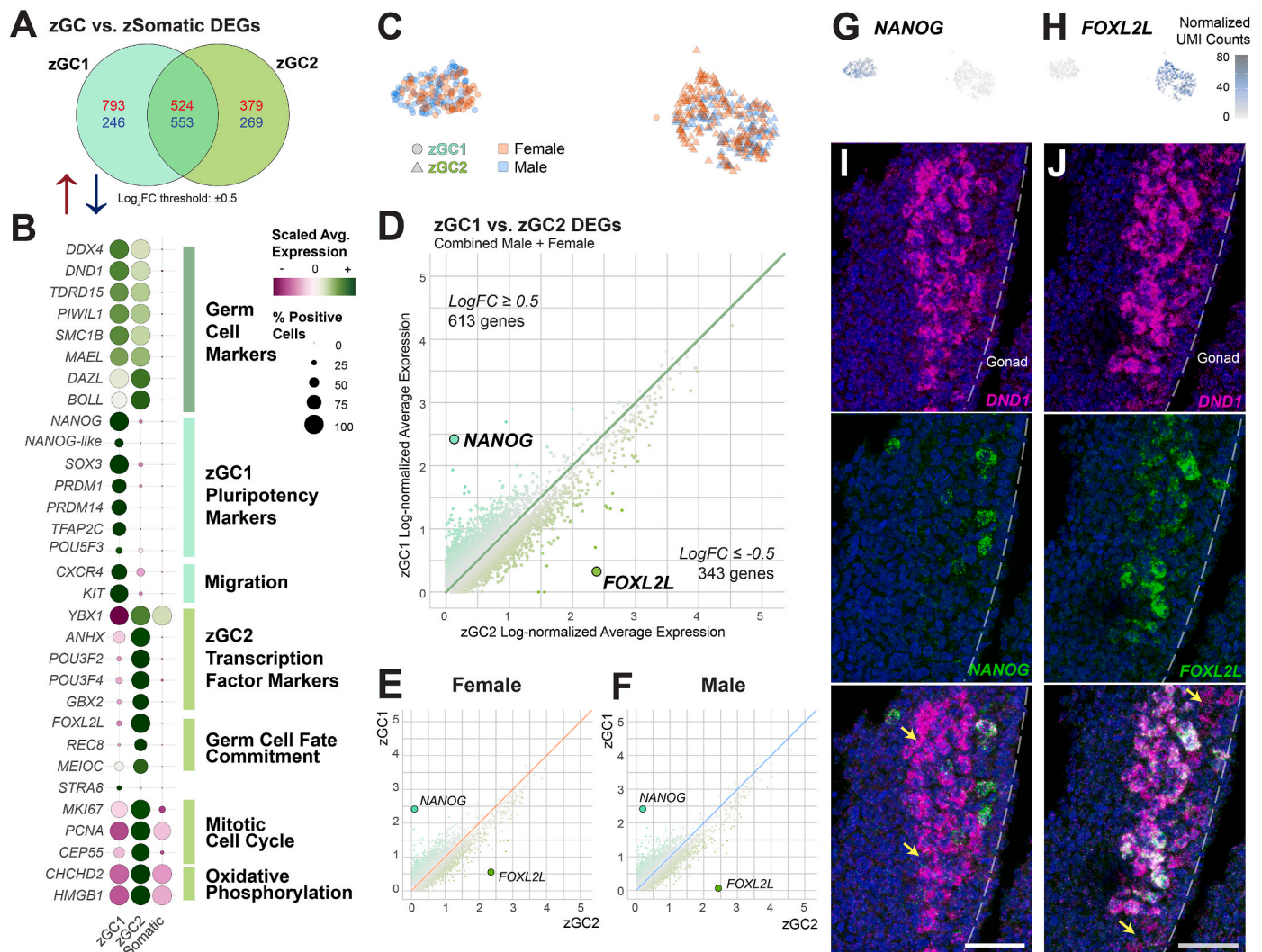


Fig. 3. Differential gene expression between the zGC clusters. 1. Venn diagram of upregulated (red) and downregulated (blue) gene expression between each zGC cluster and all zebra finch somatic cell types (zSomatic). Differential expression gene (DEG) threshold is defined as a log-fold change cutoff at ± 0.5 , percent expressing cells $>10\%$, and an adjusted p-value ≤ 0.05 . 2. Dotplot of select gene marker scaled expression between zGC and aggregate zSomatic clusters, with broad gene annotations listed to the right. 3. Abridged UMAP plot of zebra finch zGCs, highlighting the corresponding cell barcode sex by color and germ cell type by shape. 4. Log-normalized gene expression of zGC1 (y-axis) and zGC2 (x-axis) clusters for each gene. Points are colored by the relative log-fold change in gene expression between clusters, with the most differential genes, *NANOG* (*LOC100230680*) and *FOXL2L* (*LOC101233936*), highlighted. 5. Log-normalized gene expression of male zGC1 (y-axis) and zGC2 (x-axis) clusters, separated by sex. *NANOG* and *FOXL2L* are highlighted. 6. Log-normalized gene expression of female zGC1 (y-axis) and zGC2 (x-axis) clusters. *NANOG* and *FOXL2L* are highlighted. 7. zGC UMAP overlaid with *NANOG* expression (transcript UMI/10,000 total cell UMIs) in each cell barcode. 8. zGC UMAP overlaid with *FOXL2L* expression (transcript UMI/10,000 total cell UMIs) in each cell barcode. 9. Dual-label *in situ* hybridization of germ cell marker *DND1* and *NANOG* in zebra finch HH28 female left gonad. Yellow arrows highlight *DND1*+ cells without *NANOG* signal. Scale bar = 50 μm . 10. Dual-label *in situ* hybridization of germ cell marker *DND1* and *FOXL2L* in zebra finch HH28 female left gonad. Yellow arrows highlight *DND1*+ cells without *FOXL2L* signal. Scale bar = 50 μm .

markers for each cell population being *NANOG* for zGC1 and *FOXL2L* for zGC2 (Fig. 3D; Tables S8 and S9), and this was consistent for each sex (Fig. 3E–F). These markers appeared mutually exclusive by UMAP (Fig. 3G–H). We assessed these markers *in vivo* by fluorescent dual-label *in situ* hybridization on transverse sections of the zebra finch HH28 gonads, finding incomplete co-localization of *NANOG* in *DND1*+ germ cells in both sexes (Fig. 3I and S6A) and no other cell type. We noted that *NANOG* + germ cells were generally located toward the posterior and anterior ends of the gonad. Similarly, *FOXL2L* was identified exclusively in *DND1*+ germ cells (Fig. 3J–S6B and S6C), but near the center of the medial edge and tended to maintain a clustered organization. Assessments of both gonads (Figs. S6B–S6C) showed the right gonad appeared smaller in both zebra finch sexes, but especially in females, indicating the possible onset of sexual dimorphic atrophy of the right ovary by HH28 (Ayers et al., 2013). Interestingly, *FOXL2L* expression was identified in *DND1*+ germ cells in both gonads of each sex, suggesting these differentiation processes occur prior to or independently of left-right gonadal fates. This spatial expression confirmed these genes as markers of the zebra finch zGC1 and zGC2 cell types, respectively, at HH28.

Taken together, these gene expression findings imply that the zGC1 cluster is in a stem cell state, while zGC2 is in a fate determination and proliferative expansion state. This heterogeneous state exists in both sexes. In the broader context of germ cell developmental stages across vertebrates, we infer zGC1 as being gonadal PGCs and zGC2 as premeiotic gonial progenitor cells, respectively falling on earlier or later gametogenic timepoints.

2.4. Sex-biased gene expression in zebra finch gonadal germ cell clusters

While we found that differences between zGC1 and zGC2 were not due to sex differences (Fig. 3C and S2C), further analyses revealed some minor sex differences within each population (Fig. S7A). Interestingly, there were twice as many DEGs between male and female zGC1 ($n = 203$) than zGC2 ($n = 102$; Fig. S7A; Tables S10 and S11), despite zGC2 expressing more canonical markers of differentiation that corresponds with sexual fate determination. Many of these sex DEGs were found on the Z and W sex chromosomes (zGC1: $n = 85$; zGC2: $n = 67$). Nonetheless, there were fewer DEGs between sexes than those found between the zGC clusters (956 DEGs; Table S6) and several of the top zGC markers were expressed in both sexes at roughly equal levels (Fig. S7B).

2.4.1. Re-analysis of an independent dataset supports two germ cell populations

A previously published study (Jung et al., 2021) using single-cell datasets of male and female zebra finch embryonic gonads at HH28 identified three “PGC subtypes” that they defined as: 1) high pluripotency; 2) high germness; and 3) low germness/pluripotency. We sought an explanation for the differences of the number of clusters and their cell type substates between studies. As their analysis did not incorporate several standard quality controls that we used here, we reprocessed their dataset samples (denoted Seoul National University (SNU) relative to our Rockefeller University (RU) dataset) before and after applying much of our quality control workflow. Indeed, when we incorporated ambient RNA removal and mitochondrial genome mapping, but only removed cells expressing ≤ 200 genes as in their study, we actually inferred four (instead of two or three) germ cell clusters (c13, c17, c22, c29; Fig. S8A). However, we noted a bimodal distribution in summary statistics of the SNU datasets (Fig. S8B), and that clusters c13 and c29 had much lower UMI and gene counts than the other two clusters, and c29 additionally had high mitochondrial gene expression (Fig. S8C). When we applied the appropriate quality control filters (Table S1), 39.4% of the SNU cell barcodes were removed (compared to 14.9% equivalently removed in our RU dataset; Figs. S8E–S8F), and among the removed barcodes labeled as germ cells, most were derived from the c13 and c29 clusters (Fig. S8G). A large portion of removed cells were erythrocytes (Fig. S8E).

After this quality control filtering of the SNU dataset, the remaining cells generated a UMAP landscape of gonadal cell types similar to our dataset (Fig. S9A; Table S12). Importantly, this analysis left only two germ cell clusters remaining, primarily made up of barcodes from c17 and c22 in the unfiltered dataset (Fig. S8G); now labeled as c10 and c25 in the filtered dataset (Fig. S9A). A comparative reference-query mapping and label transfer analysis (Stuart et al., 2019) of the filtered SNU dataset to the filtered RU dataset showed high concordance between expression profiles of the clustered cell types (Fig. S9B). The c10 and c25 SNU filtered dataset analyses matched the distinct zGC1 and zGC2 clusters of the RU dataset. Importantly, we found similar DEG markers for these clusters (Fig. S9B; Table S13), and similar module score enrichments for the candidate GRC gene paralogs in the SNU zGC populations (Fig. S9D; Table S7). These findings across independently generated scRNAseq datasets support two distinct but closely related clusters in the zebra finch gonad at HH28.

2.5. Single-cell transcriptomic analysis identifies one germ cell population in the HH28 chicken gonad

To compare zebra finch and chicken, we generated scRNAseq datasets from male ($n = 2$) and female ($n = 2$) chicken embryonic gonads at HH28, a stage where chicken PGCs are commonly collected for reproductive technology applications (Choi et al., 2010). This stage is just prior to the sexual differentiation of developing chicken gonads at HH29 (Ayers et al., 2015; Estermann et al., 2020b). The chicken samples were processed simultaneously and with the same quality control steps as the zebra finch samples (Fig. S10; Table S1). A total of 8607 cells were mapped against a chicken reference genome with 24,180 gene annotations (GCF_000002315.6; Table S14) and visualized by UMAP (Fig. 4A; Table S15). Clustered cell types were identified through nearest-neighbor clustering and marker-based label transfer (Fig. 4B). Between chicken datasets we noted a higher total number of female cells than male, but cell type proportions between sexes remained roughly equivalent (Fig. S10D). These cell types were similar to those found in the zebra finch, as they broadly shared many of the same gene markers (Figs. 4C and 1D; Table S14).

In contrast to the zebra finch, only one chicken germ cell (cGC) cluster was found (c17, Fig. 4A–C) and it remained stable across multiple clustering resolutions (Fig. S10B). An assessment of DEGs between cGCs and chicken somatic (cSomatic) cells marked the cGC cluster with 1049-up regulated and 380-down regulated genes. The up-regulated genes included many canonical PGC markers, such as *NANOG*, *POU5F3* (*OCT4* homolog), and *KIT* (Fig. S11A; Table S16). Between the male and female chicken cGC clusters there were fewer DEGs ($n = 59$; Fig. S11B; Table S17) than between sexes for either zGC cluster, and about half of these genes were located on the sex chromosomes ($n = 27$). To validate a unitary PGC population, *in situ* hybridization revealed a complete overlap of *DAZL* and *NANOG* in HH28 chicken gonads and dorsal mesentery (Fig. S12). Consistent with prior studies (Rengaraj et al., 2022), these results support the presence of just one germ cell state in the chicken gonad at HH28, which we identify as gonadal PGCs.

2.6. Comparison of chicken and zebra finch HH28 gonadal germ cells

To directly compare the chicken and finch HH28 gonadal cells, we integrated the processed RU datasets using 13,913 identified orthologous gene pairs between species (Tables S2 and S14). A reference-query label transfer analysis of the clustered cell types showed good mapping between interspecific cell types (Fig. 5A and S13A); though the Mesenchymal “supercluster” (IM Progenitors, Pre-Granulosa/Sertoli and Theca/Leydig cell types) showed lower overlap between species. Of note was a higher proportion of IM progenitor cells versus pre-Sertoli and Granulosa cells in the chicken compared to the zebra finch (Fig. 5B), matching previously published findings (Estermann et al., 2021). Other cell types of each species, such as the endothelial and epithelial cell

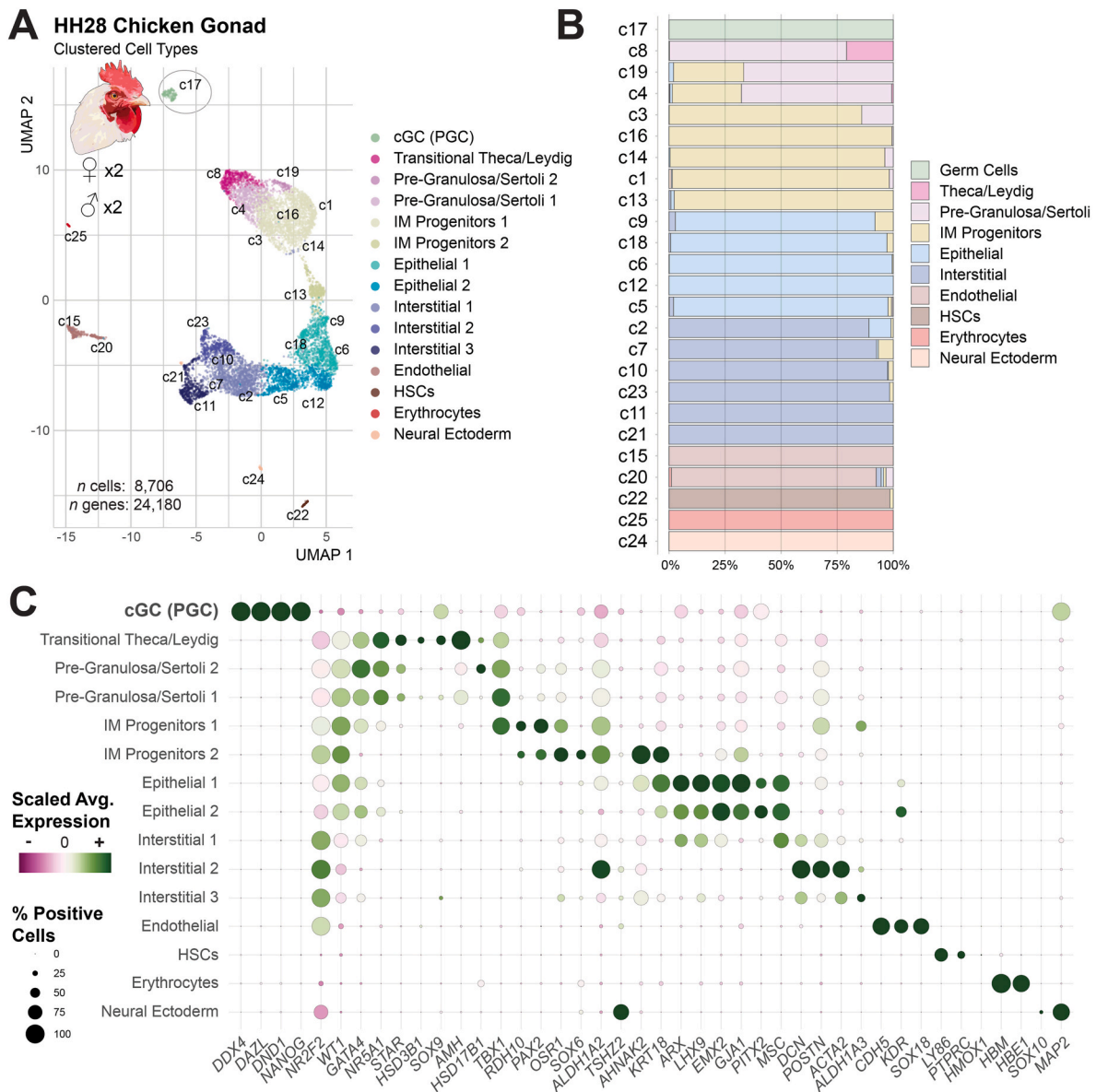


Fig. 4. The chicken HH28 gonad has only one germ cell cluster. **A.** UMAP plot of male and female chicken gonadal at HH28. Cells are colored by the clustered cell type, with initial nearest-neighbor cluster labels overlaid. Further information on quality control and dimensional reduction for this dataset may be found in [Figure S10](#). **B.** Proportional bar chart of inferred cell types in each nearest-neighbor cluster. **C.** Dotplot of scaled expression for select gene markers of each clustered cell type identified in the HH28 chicken gonad.

clusters, largely conformed to roughly equivalent general UMAP coordinates ([Fig. 5B](#)).

The chicken cGC clustered with the zebra finch zGCs rather than with the other somatic cell types ([Fig. 5A](#)), and we noted on the integrated UMAP that the chicken cGC occupied an intermediate position between zGC1 and zGC2 ([Fig. 5B](#) and [S13A](#); [Table S18](#)). However, nearest-neighbor clustering of the integrated species dataset identified two germ cell clusters, c20 and c21, with c20 primarily composed of both cGC and zGC1 cells and c21 almost exclusively of zGC2 cells ([Figs. S13B–S13D](#)). Examining individual DEGs between germline and species-specific somatic clusters ([Fig. 5C–H](#)), both zebra finch and the single chicken germ cell populations shared many marker genes ($n = 325$; [Fig. 5C](#)), including *DND1*, *DDX4*, and *DAZL* ([Fig. 5D](#); [Table S19](#)). Consistent with the clustering analyses, the cGC and zGC1 populations shared upregulated gene expression of many pluripotency markers, including *NANOG*, *SOX3*, *PRDM1*, *PRDM14*, and *TFAP2C* ([Fig. 5E](#)) ([Chambers et al., 2007](#); [Jean et al., 2015](#); [Magnúsdóttir et al., 2013](#);

[Motono et al., 2008](#)), migratory markers *CXCR4* and *KIT* ([Lee et al., 2017](#); [Srihawong et al., 2016](#)), as well as the spermatogonial stem cell marker, *GFRA1* ([Buageaw et al., 2005](#)). cGC cells also expressed a few genes upregulated in the zGC2 population, such as *POU3F2* and *DLX2*, and several cell cycle genes, such as *CDCA3* and *CCT2* ([Fig. 5F](#)).

In addition to cell identity markers, we identified several growth factor receptor similarities and differences between the three germ cell populations. In all three populations (cGCs, zGC1, and zGC2), there was consistent upregulation of several SMAD and TGF- β superfamily signaling receptors (*ACVR2B*, *SMAD5* and *SMAD3*; [Fig. 5G](#)), though *ACVR2B* and *SMAD5* were more highly expressed in zGC2 than zGC1 ([Table S6](#)). However, compared to the cGC cluster, zGC2 demonstrated poor expression of *SMAD1*, and zGC1 demonstrated downregulation of receptor subunit genes *ACVR1* and *BMPRIA*. These findings suggest that BMP and Activin signaling within the TGF- β superfamily, necessary for the maintenance and self-renewal of migration-competent chicken PGCs ([Whyte et al., 2015](#)), may have divergent roles in zebra finch germ

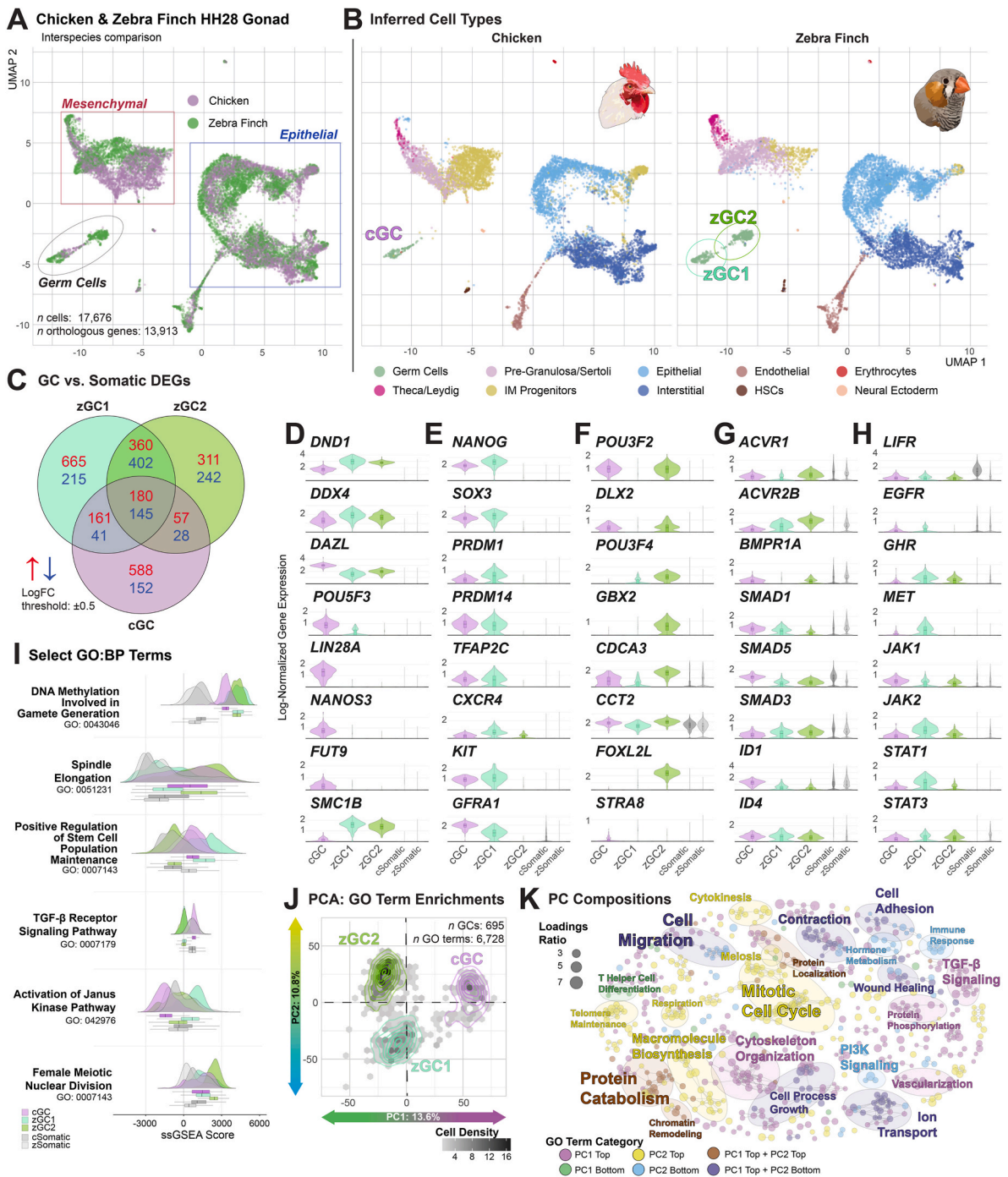


Fig. 5. Comparison of chicken and zebra finch HH28 germ cell clusters. 1. UMAP plot of integrated chicken (purple) and zebra finch (dark green) gonadal datasets at HH28. 2. Separation of the integrated UMAP in subfigure A by species and colored by inferred cell type. 3. Venn diagram of upregulated (red) and downregulated (blue) gene expression between each GC cluster and species-respective somatic cell types. A differential expression threshold is defined at a log-fold change of ± 0.5 . 4. Violin plots of log-normalized gene expression between GC clusters from each species. Aggregate somatic expression for chicken (cSomatic) and zebra finch (zSomatic) are provided in grey. I. Ridge plots of select GO Terms, showing relative single-sample gene set enrichment analysis (ssGSEA) scores between GC and somatic cell populations. J. Projection of Principal Component Analysis (PCA) for all GO Term enrichments assessed for each GC cluster. K. EMAP Plot highlighting principal component GO Term loadings connected by Jaccard score. See Table S21 for cluster compositions.

cell development.

We noted some clear species differences. Several well-characterized chicken germ cell markers, *POU5F3*, *LIN28A*, *NANOS3*, and *FUT9* (an SSEA-1 epitope synthesis gene) had low or absent expression in both zebra finch zGC1 and zGC2 (Fig. 5D). Conversely, *SMC1B*, a previously identified zebra finch germ cell marker (Jung et al., 2021), was found in both zGC clusters, but low in cGC (Fig. 5D). In zGC1, we also found

significant upregulation of several JAK/STAT-related receptors (e.g., *GHR*, *MET*) and downstream genes (e.g., *JAK2*, *STAT1*) not upregulated in cGC (Fig. 5H). Importantly, only zGC2 expressed fate determination markers, such as *FOXL2L* (Fig. 5F). Interestingly, zGC2 did not have significant expression of *STRA8* (Fig. 5F), an RA-stimulus response gene canonically signaling the onset of meiotic fate determination in chicken (Smith et al., 2008). To ensure that the absence of expression was not

due to annotation error, raw read alignments for several orthologs with species-specific expression were manually reviewed against their respective genome references (Fig. S14). We found no evidence of annotation or other error to explain these species differences.

We wondered whether the cGC cluster shared any expression with the identified GRC gene paralogs, as found in the zGC clusters. We scored gene modules composed only of zebra finch GRC gene candidates with chicken paralogs ($n = 69$) and saw no major enrichment in cGC vs. cSomatic clusters ($\text{Log}_2\text{FC} < 0.5$; Fig. S15A; Table S7). The zebra finch module enrichments were similar between the orthologous geneset and the full geneset (Figs. S15B and 2C). In particular, we also found that chicken *NAPA* was not upregulated in cGC vs. cSomatic clusters, like zebra finch *NAPA_A* but not *NAPA_{GRC}* (Fig. S15C). Altogether these results imply that zebra finch GRC genes provide unique germline expression patterns not demonstrated by either the zebra finch A chromosome paralogs or chicken A chromosome orthologs.

2.7. Functional gene category differences between zebra finch and chicken primordial germ cells

To assess broader functional characteristics between the germ cell populations, we ran single-sample gene set enrichment analysis (ssGSEA) against 6728 Biological Process Gene Ontology terms (GO; Aleksander et al., 2023) containing more than five zebra finch/chicken gene orthologs (Table S20). As expected, each germ cell cluster was enriched for several germ cell-related GO terms compared to gonadal support cell populations, including “DNA Methylation Involved in Gamete Formation” (Fig. 5I). Other GO terms were highly differential between each cell type, including cell polarity and cell adhesion terms (Fig. S16A), which are both related to PGC migration (Richardson, 2010). The cGC population appeared more enriched for these terms, while zGC1 and especially zGC2 appeared the less enriched, and select marker gene analysis corresponded to these enrichments (Figs. S16B–S16C). Compared to somatic cell enrichments, mitosis-associated genesets (e.g., “Spindle Elongation”) were enhanced in zGC2 and cGC, while terms such as “Positive Regulation of Stem Cell Population Maintenance” were enhanced in zGC1 and cGC (Fig. 5I). Interestingly, cGCs but not zGCs were enriched for “TGF-beta Receptor Signaling Pathway” compared to their corresponding somatic cells, whereas zGC1 was exclusively enriched for “Activation of the Janus Kinase Pathway,” mirroring the individual DEG observations. Only zGC2 was enriched for terms related to the developmental progression and differentiation of the germline (e.g., “Female Nuclear Meiotic Division”).

We applied PCA for all GO enrichment scores for the germ cell populations across 694 PCs (Table S21). PC1 and PC2 accounted for 13.6% and 10.8% of the variation, respectively (Fig. 5J). PC1 primarily acted to delineate species differences, while PC2 separated the zGC1 and zGC2 populations (Fig. 5J). More than 90% of the total variance was accounted for by PC3–PC375, though none individually accounted for more than 4% of the total variation.

To identify larger trends between the three germ cell populations, GO terms contributing most to PC1 and PC2 were projected onto an enrichment map, and clustered by Jaccard similarity. The identified PC1 terms had a notable right-sided contribution bias (355 positive terms; 14 negative terms) and had broad enrichment categories differences in TGF- β superfamily signaling, vascularization, and cytoskeletal organization (top quadrant) and T helper cell differentiation (bottom quadrant; Fig. 5K; Table S22). Terms on the opposing ends of PC2 (231 positive terms; 121 negative terms) resolved clusters broadly defined by mitotic cell cycle (top quadrants), macromolecule biosynthesis terms, and cell migration (bottom quadrants). We also saw cluster differences for GO terms involved in JAK/STAT, PI3K/AKT, and WNT signaling pathways. Overall, these species and germ cell type functional differences support a distinction in all three populations and highlight the complex and dynamic nature of germ cell populations in avian embryonic gonads.

2.7.1. Cross-species functional analysis of gonadal somatic cells

Considering the developmental differences between chicken and zebra finch germ cell clusters, we sought to assess functional differences of particular extrinsic signaling pathways in the developing gonadal somatic cells. We found species differences in gene expression between markers of sex hormone biosynthesis (Fig. S17). Namely, the zebra finch mesenchymal cell “supercluster” (Fig. S17A), and to a lesser extent the epithelial supercluster, showed upregulated expression of sex hormone synthesis genes (Fig. S17B). Compared to chicken, the *HSD3B1* progesterone biosynthesis enzyme gene was elevated in zebra finch mesenchymal and epithelial clusters. ssGSEA highlighted an enrichment of “Progesterone Biosynthetic Process” (GO: 0006701) in zebra finch somatic clusters compared to chicken (Fig. S17C). Germ cells of both species expressed the nuclear progesterone receptor (*PGR*) and several membrane progesterone (*PAQR3*, *PAQR8*) receptor genes (Fig. S17D). The *HSD17B1* redox enzyme gene that enhances androgen and estrogen potency was also elevated in zebra finch clusters, though androgen and estrogen receptors were not highly expressed in any zGC or cGC clusters at this stage. Only the female zebra finch mesenchymal support (pregranulosa) cell clusters expressed *CYP19A1*, which converts testosterone to estrogen. These hormones have critical roles in sex determination of the developing avian gonad (Ayers et al., 2013; Clinton and Zhao, 2023; Smith et al., 2009).

We identified differences for retinoic acid (RA) signaling (GO: 0042573 “Retinoic Acid Metabolic Process”), which was more highly enriched in chicken somatic cells compared to zebra finch (Fig. S18A). Indeed, compared to zebra finch, chicken somatic cells demonstrated higher gene expression of *ALDH1A2*, whose protein product converts retinaldehyde into RA, and lower levels of the *CYP26B1* retinoic acid degradation gene (Fig. S18B). Interestingly, while *STRA8* was absent in all germ cell clusters (Fig. 5F), both zGC clusters showed higher expression of several RA signaling and stimulus response genes not elevated in the cGC cluster (e.g., *OPN3*, *RBP5*, *STRA6*, *RARB*; Fig. S18C).

These findings suggest that the somatic cells of the zebra finch gonad begin sexual differentiation of the gonads by HH28, consistent with histological observations of distinct morphological and symmetrical differences between the female and male zebra finch gonads (Figs. S6B–S6C). Interestingly, this differentiation occurs despite major sex differences in germ cell gene expression (Fig. S7). In contrast, chicken gonads remain in a bipotential state at HH28, prior to ovarian or testicular commitment starting at HH29 (Ayers et al., 2015; Estermann et al., 2020a, 2020b; Smith et al., 2008). Interestingly, the expression patterns of RA biosynthesis and response genes suggest key species differences in the sensitivity and timing of RA signaling in gonadal development between chicken and zebra finch.

2.7.2. Gonadal *FOXL2L* expression occurs in zebra finch as early as HH25

We sought to further assess zebra finch germ cell heterogeneity *in vivo* across multiple stages of gonadal development through dual-labeling of *NANOG* and *FOXL2L*. In addition to both male and female zebra finch HH28 gonads, each germ cell marker could be distinguished in cells, without co-localization, at earlier (HH25) and later stages (HH36; Fig. 6A–C), documenting germ cell heterogeneity at multiple developmental timepoints. This finding at HH25 was particularly unexpected, as *NANOG* + PGCs were still found in the dorsal mesentery (DM) and potentially migrating toward the gonadal ridge. This was further supported by incomplete co-localization of *DND1* + germ cells with *NANOG* (Fig. S19) or *NAPA_{GRC}* (Fig. S20) at this stage. In sections of HH36 zebra finch gonads, we generally saw many more *FOXL2L* + cells than *NANOG* + cells (Fig. 6D and E), though each marker could be identified in both sexes. These data suggest that the activation of *FOXL2L* expression readily occurs upon zebra finch germ cell settlement into the gonadal ridge, and that the proportion of these cells increases and persists until at least HH36.

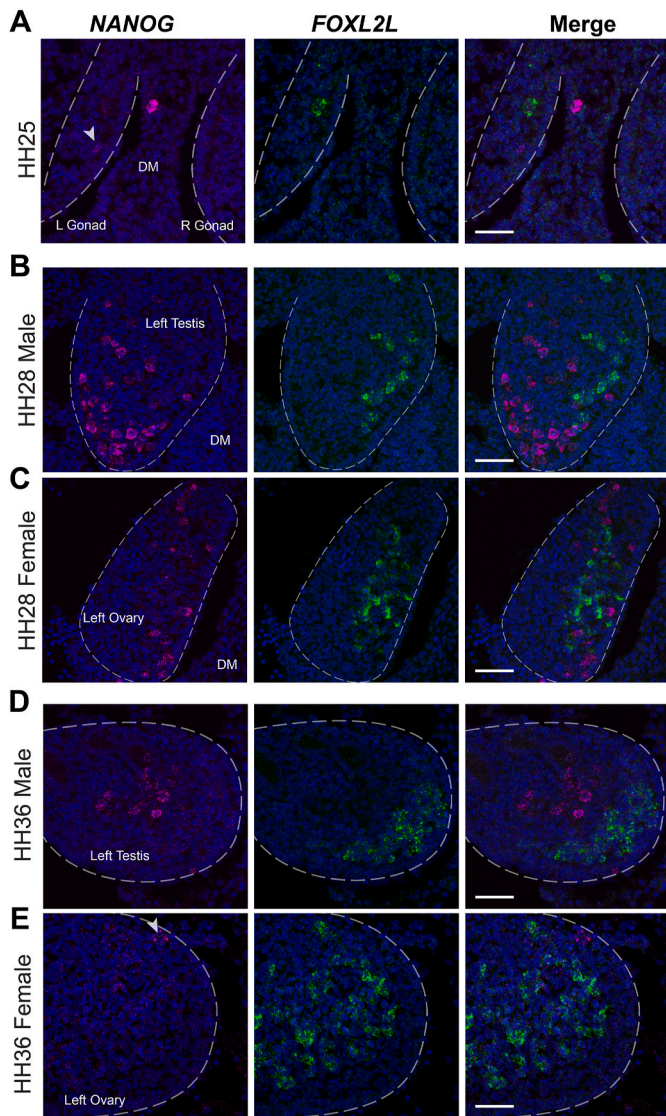


Fig. 6. Zebra finch germ cell heterogeneity across gonadal development. 1. Dual-label *in situ* hybridization of *NANOG* and *FOXL2L* in HH25 gonads. Arrowhead denotes *NANOG* signal in gonad. 2. Dual-label *in situ* hybridization of *NANOG* and *FOXL2L* in HH28 male gonads. 3. Dual-label *in situ* hybridization of *NANOG* and *FOXL2L* in HH28 female gonads. 4. Dual-label *in situ* hybridization of *NANOG* and *FOXL2L* in HH36 male gonads. 5. Dual-label *in situ* hybridization of *NANOG* and *FOXL2L* in HH36 female gonads. Arrowhead denotes *NANOG* + signal in gonad.

2.8. Zebra finch germ cell heterogeneity parallels that of HH36 chicken females

To compare gonadal germ cell differentiation between species and potentially identify similar gene expression profiles to zGC2 in chicken, we utilized previously published scRNAseq datasets of chicken embryonic gonadal development where germ cell expression patterns had not been extensively explored (Estermann et al., 2020a, 2020b; denoted as MU for Monash University). We processed the MU datasets using our analysis workflow to assess germ cell development across multiple timepoints: HH25 (their embryonic day 4.5 (E4.5)), HH30 (E6.5), HH35 (E8.5), and HH36 (E10.5; Fig. S21; Table S23). To assess the batch comparability of the RU and MU datasets, we compared our RU HH28 chicken datasets to the closest MU time point, male and female HH30. We found that our inferred cell type classifications largely matched the somatic cell type classifications used by the MU study

(Figs. S22A–S22B). The mesenchymal supercluster showed less distinct similarities, with the HH30 IM progenitor population much smaller proportionally than that found at HH28 (Fig. S22B). This analysis concurs with the known timing (HH29; Ayers et al., 2015) of sexual differentiation in the chicken gonad.

Notably, in an aggregate of all MU datasets as well as for each male and female chicken gonadal time point, our analyses resolved only one cluster of germ cells (Figs. S21B–S21C). cGCs showed progressive declines in gene expression of several stem cell markers (e.g., *NANOG*, *PRDM14*, *LIN28A*), though measurable expression only persisted in the male HH36 gonadal dataset (Fig. 7A). In contrast, several genes showed differential expression patterns between female HH35 and HH36 germ cells (Fig. 7A; Table S24), corresponding with the RA-mediated onset of oogenesis in chicken around this developmental stage (Rengaraj and Han, 2022; Smith et al., 2008). The loss of *NANOG* and other pluripotent markers coincided with *FOXL2L* expression in female HH36 germ cells, matching the known onset of *FOXL2L* upregulation in the left gonad of female chicken embryos at E9 (Ichikawa et al., 2019).

As only one cluster of chicken germ cells was derived at each stage, we sought to discern any germ cell heterogeneity within the HH36 scRNAseq datasets. By individually subclustering the HH36 chicken germ cells for each sex, we resolved two female germ cell clusters that we denoted as fcGC1 and fcGC2 (Fig. 7B; f for female). In contrast, the male cells still formed only one *NANOG* + cluster (mcGC1; Fig. 7B; Table S25). The female clusters were distinguished from cSomatic clusters and each other by several markers, notably *NANOG* (fcGC1) and *FOXL2L* (fcGC2) (Fig. 7C–E and S23A; Tables S25–S27). Dual-label *in situ* hybridization validated these patterns in chicken HH36 gonads, showing regional exclusivity of *NANOG* and *FOXL2L* gene expression in *DND1*+ cells (Fig. 7F–G and S24A), as these populations appeared restricted to the interior or ventral edge of the developing gonad, respectively. Anecdotally, this localization was in contrast with *FOXL2L* + germ cells in the HH36 zebra finch ovary, appearing largely restricted to the medulla (Fig. 6E). *FOXL2L* was not expressed in male HH36 gonads (Fig. S24B), nor at earlier chicken gonadal stages (Figs. S24B–S24D). Between male and female cGC1 clusters at HH36, there were relatively few other genes demonstrating high log-fold change differences, with much of the differential expression coming from sex-chromosome genes (Fig. S23B; Table S28).

Between the female fcGC1 and fcGC2 clusters, several differential markers mirrored those found between the zGC1 and zGC2 clusters (Fig. 7H; Table S29). In particular, transcription factors *NANOG* and *SOX3* were highly conserved markers for the zebra finch and chicken female GC1 cluster, while *FOXL2L* and *HMGB1* were consistently upregulated in the female GC2 cluster of both species. Between fcGC1 and fcGC2, several TGF- β /SMAD superfamily signaling pathway genes declined, including those upregulated between zGC1 and zGC2 such as *ACVR2B* and *SMAD5* (Fig. 7H). As in the HH28 cGC cluster, JAK/STAT signaling pathway genes were lowly expressed or absent in both fcGC clusters at this stage (Fig. 7H). Orthologous GRC gene candidates were also expressed at low levels (Fig. 7H), and orthologous GRC module scores also did not demonstrate significant enrichment in the MU cGC clusters (Fig. S25; Table S7).

To comprehensively assess corresponding similarities between the chicken and finch germ cell types, we compared the gene expression profiles of all orthologous genes between HH28 zGCs and HH30–36 cGCs by reference mapping analysis. Similarities scores for each zGC–cGC grouping showed male and female zGC1 were diffusely similar to multiple male and female cGC timepoints from HH30 and HH35, but generally paired most closely with cGC populations of their respective sex (Fig. 7I; Tables S30 and S31). In contrast, both the male and female zGC2 populations mapped most closely to female HH36 cGC2 cells. Similar results were found for the zGC clusters in the SNU dataset (Fig. S26A; Tables S31 and S32). As a control, an equivalent analysis using the RU chicken datasets mapped the HH28 cGC cells across either MU cGC1 cluster favoring the corresponding sex (Fig. S26B; Tables S31

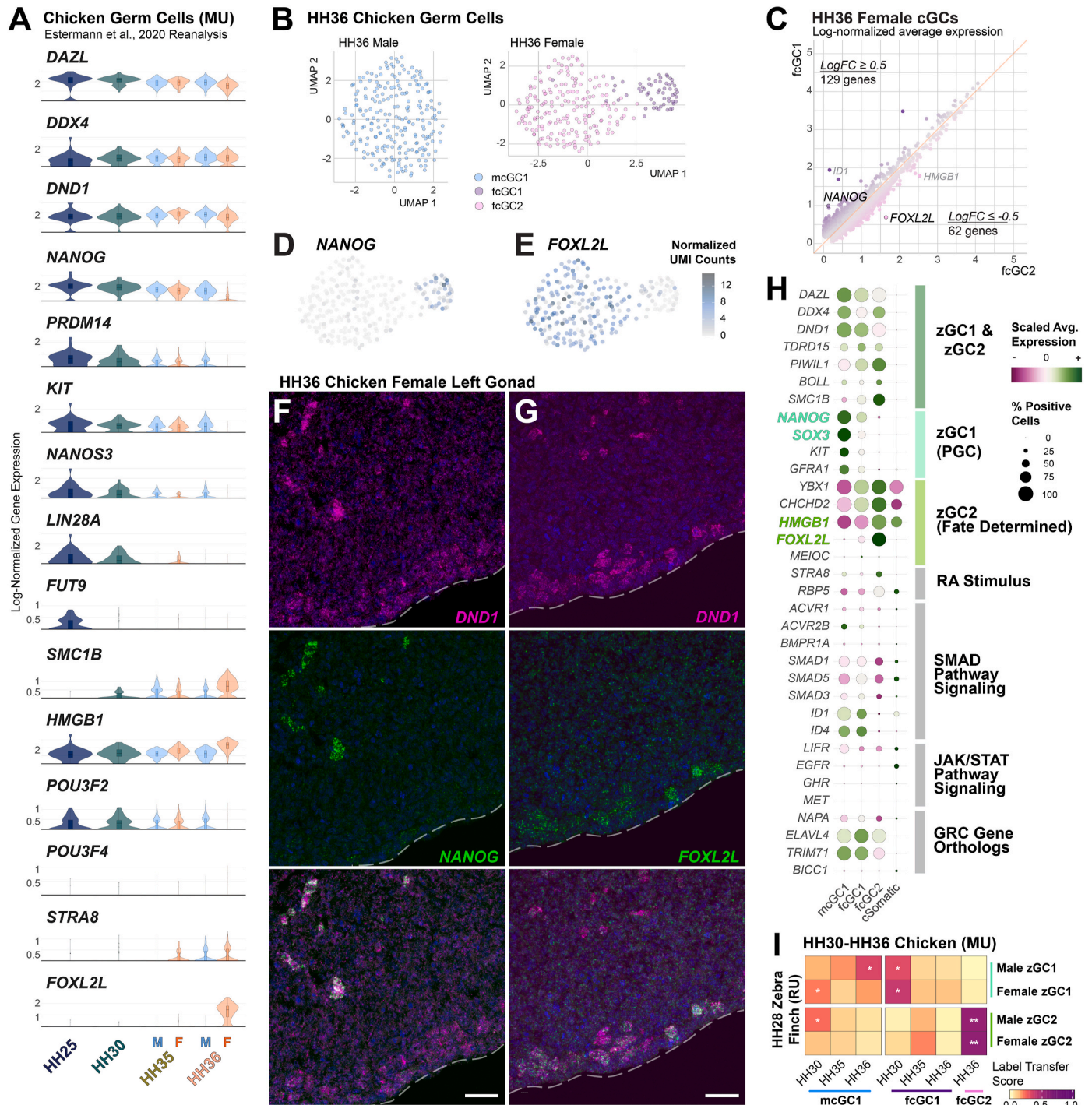


Fig. 7. Chicken germ cell heterogeneity in later embryonic development. 1. Violin plots of select genes in male and female chicken gonadal germ cells on different embryonic days. 2. Independent subclustering of male and female HH36 chicken germ cells. Note the one cluster resolved in the male dataset vs. the two clusters in the female dataset. 3. Comparison of average log-normalized gene expression between fcGC1 (y-axis) and fcGC2 (x-axis). A selection of the highest log-fold change genes are labeled. 4. HH36 Female cGC UMAP overlaid with *NANOG* expression (transcript UMI/10,000 total cell UMIs) in each cell barcode. 5. HH36 Female cGC UMAP overlaid with *FOXL2L* expression (transcript UMI/10,000 total cell UMIs) in each cell barcode. 6. Dual-label *in situ* hybridization of germ cell marker *DND1* and *NANOG* in chicken female HH36 gonads. Scale bar = 50 μ m. 7. Dual-label *in situ* hybridization of germ cell marker *DND1* and *FOXL2L* in chicken female HH36 gonads. Scale bar = 50 μ m. 8. Dotplot of select gene marker scaled expression between E10.5 male and female cGCs and aggregate cSomatic clusters. Gene symbols highlighted by color correspond to zGC1 (teal) or zGC2 (lime) marker conservation. 9. Confusion matrix of label transfer similarity scores for male and female zebra finch zGC clusters (RU) against chicken (MU) germ cells at HH30, HH35, and HH36. A $\log_2FC > 0.50$ against other MU stage scores and a $p\text{-value} \leq 0.05$ by one-sided *t*-test is denoted by *. A $\log_2FC > 2.0$ is denoted by **.

and S33). Collectively, these data show that although chicken PGCs form a relatively uniform population during embryonic development, by HH36 female chicken germ cells begin to segregate into two populations that have similarities to the two finch populations found throughout development.

3. Methods

3.1. Animal husbandry and sources

Animals were cared for in accordance with the standards set by the American Association of Laboratory Animal Care and Rockefeller University's Animal Use and Care Committee. Zebra finches were maintained under a 12:12-h light/dark cycle at 18–27 °C and breeding pairs provided with a finch seed blend, millet spray, egg mash with fresh squeezed oranges daily, and fresh fruits and vegetables once to twice weekly. A hanging nest box and *ad libitum* jute/cotton mix for nesting material were placed in each cage. Eggs were collected daily and stored at 16–18 °C, 80% humidity for up to 7 days. Fertile White Leghorn chicken eggs were obtained from Charles River Laboratories.

3.2. Embryo sexing

Chicken and zebra finch eggs were incubated at 37 °C, 60–70% humidity; zebra finch eggs were additionally incubated with intermittent rocking (Showa Furanki). On day 5 of incubation, a small window (2–3 mm diameter) was made in the eggshell of zebra finch eggs, which usually produced a small bleed. Blood was absorbed using Whatman filter paper or a glass needle and then placed into Chelex 100 (Bio-Rad). Chicken eggs were windowed (1 cm diameter) and 1–2 µL blood collected using a glass needle inserted into a vitelline vein. Eggs were resealed with Scotch tape (chicken) or paraffin (zebra finch) and returned to the incubator. DNA was isolated from the blood samples using manufacturer's instructions for Chelex 100 and sexotyping was performed by amplifying the *CHD* genes (primers P2: TCTGCATCGC-TAAATCCTTT; P8: CTCCCAAGGATGAGRAAYTG) with a previously published Taq-polymerase PCR protocol (Griffiths et al., 1998).

3.3. Single-cell collection

On day 6, HH28 embryos were removed from eggs. Gonad pairs were dissected from the embryos using fine forceps and then placed in room temperature 0.05% trypsin-EDTA. Whole gonads were incubated in trypsin for 5 min (zebra finch) or 15 min (chicken) at 37 °C and then dissociated by gently pipetting up and down with a p200 pipette until cell clumps were no longer visible. Trypsin was inactivated with an equal volume of PGC cell culture media containing 10% FBS (Jung et al., 2019). For the *in vivo* gonad samples, gonads from two embryos were pooled to create each sample, and four total samples were collected: chicken male and female, and zebra finch male and female. The resulting cells were washed with PGC media and run through a 40 µm filter to remove any remaining cell clumps. Samples were resuspended in PGC media and counted using the ThermoFisher Countess II Automated Cell Counter (AMQAX1000) with DAPI vital staining. The following cell counts were obtained for each pooled sample: chicken female ~700 cells/µl, chicken male ~1600 cells/µl, zebra finch female ~2000 cells/µl, zebra finch male ~2100 cells/µl. Greater than 96% of the cells in each sample were alive.

3.4. Single-cell capture on 10x genomics chromium

A single Chromium microfluidic Chip B (10x Genomics #2000060) was prepared by pipetting 50% glycerol into all unused wells. A Reverse Transcriptase Master Mix was prepared following the manufacturer's protocol (Chromium Single Cell 3' Reagent Kit v3) and was split into four aliquots. Appropriate volumes of water and cell suspension were added

to the Master Mix to capture an estimated 7000 cells for each sample. 10x Genomics v3 GEM Beads (#2000059) and Partitioning Oil (#220088) were then pipetted into the microfluidic chip following manufacturer's protocol, and a droplet emulsion was created on the chromium instrument. The emulsion was incubated at 53 °C for 45 min to allow for reverse transcription and heat deactivated at 85 °C 5 min. Emulsion was then broken and cDNA amplified according to manufacturer's protocol, and the resulting cDNA was measured on a Qubit Fluorometer (ThermoFisher #Q33238). cDNA quantification was as follows: chicken female 12.1 ng/µl, chicken male 17.62 ng/µl, zebra finch female 34.6 ng/µl, zebra finch male 29.6 ng/µl. The resulting cDNA was also visualized on the Agilent Fragment Analyzer (#M5310AA) using the High Sensitivity NGS Kit (#DNF-474-0500) to confirm cDNA size range and primer-dimer prevalence.

3.5. Illumina library preparation and sequencing

cDNA samples were diluted to either 50 ng (chicken) or 100 ng (zebra finch) and were used as input into library preparation for Illumina sequencing following the 10x Genomics protocol (Chromium Single Cell 3' Reagent Kit v3). Illumina libraries were quantified using a Qubit Fluorometer (#Q33238) and visualized using an Agilent Fragment Analyzer (#M5310AA, DNF-474-0500). The following quantifications were obtained for the samples: chicken female 22ng/ul; chicken male 27.2 ng/ul; zebra finch female 34 ng/ul; zebra finch male 32 ng/ul. Libraries were labeled using the Chromium i7 Multiplex Kit (PN-120262) and sequenced on either an Illumina HiSeq 4000 or NovaSeq S4 (pair-ended with read lengths of 150 nt) for approximately 2 billion reads per sample.

3.6. Reference genome curation dataset processing

The reference genome and annotation files were downloaded from NCBI (zebra finch: GCF_003957565.2; chicken: GCF_000002315.6). Using previously generated bulk RNAseq datasets, the UTR regions were predicted and added to the annotation file by invoking StringTie (ver 2.1.7). Reference files were built by Cellranger (ver 6.0.1, 10X genomics) mkref command with the polished annotation file, reads were aligned and counted by cellranger count command. Ambient RNA ratios were estimated and cleaned by R package SoupX (Young and Behjati, 2020).

Orthologous gene pairs between zebra finch and chicken were identified using BioMart, eggNOG (Huerta-Cepas et al., 2018), reciprocal tBLASTx, and identical gene symbols. All the orthologous genes are listed in (Tables S3 and S12).

During post-processing analysis, the single-exon zebra finch gene LOC101233936 (*FOXL2L*) was found to be insufficiently annotated, likely due to a high GC-rich region in the 3' half of the open reading frame (ORF). The annotation was extended through the ORF where a StringTie-identified 3' UTR was present. Zebra finch datasets were then re-run against the corrected reference genome and amended LOC101233936 read counts were then added into the existing Seurat objects.

3.7. GRC gene alignment simulation

A simulated small genome was generated as a reference based on the sequence of 8 genes, in which the sequences of 4 genes (*BICC1*, *ELAVL4*, *NAPA*, *TRIM71*) were extracted from the autosomes according to the location of whole genes (UTRs, exons and introns), and the sequences of 4 genes (*BICC1*, *ELAVL4*, *NAPA*, *TRIM71*) from the mRNA sequence of the GRC. Each sequence of these 8 genes were assigned as a chromosome, and a gtf file was generated accordingly. In total, 100,000 96 bp long reads were simulated using the R package Subread based on the reference and gtf files outlined above, which produced a theoretical coverage of 298X (Liao et al., 2019). The number of reads per gene was

proportional to gene length. Cellranger was used to align the reads back to the genome, and the exon base coverage was calculated by samtools depth (ver 1.12).

3.8. Single-cell RNAseq object processing by Seurat

After ambient RNA removal, the clean matrices were loaded into the Seurat R package (version 4.3.0.1) for downstream analysis. Barcodes falling outside of selected thresholds for ambient RNA-adjusted “nCount_RNA,” “nFeature_RNA,” and the percent mitochondrial genes were removed (Table S1). Doublet droplets were predicted and removed using doubletFinder (ver 2.0.3).

Seurat objects were normalized and scaled ($n = 3000$ genes) by SCTransform (version 0.3.5; Hafemeister and Satija, 2019) with cell cycle and mitochondrial gene regression. Sample integration, dimensional reduction ($n = 50$ PCs), and nearest-neighbor cell clustering were performed using suggested parameters by the Seurat package. In the RU zebra finch HH28 data, subclustering of zGC2 further resolved clusters corresponding to erythrocytes (c11.8, $n = 15$) and a small number of cells (c11.9, $n = 12$) expressing both hematopoietic stem cell and germ cell markers (Fig. S2E); c11.9 was excluded from analyses in this study as a potential doublet artifact or an extremely rare population not found by histology (not shown).

Inferred cell types were identified by first identifying reference cells that strictly expressed canonical cell type markers (Table S2), then using Seurat’s “TransferData” function to identify the cell type identities of the remaining cells based on nearest-neighbor similarity. Clustered cell types were determined by the majority inferred cell type within nearest-neighbor clusters and similar clusters were aggregated using Seurat’s “BuildClusterTree” function. Data visualizations were performed using Seurat functions and modified using ggplot2 commands prior to figure generation in Adobe Illustrator (version 27.5).

Differentially expressed genes were called by the Seurat functions “FindMarkers.” Similarity matrices were generated using the Seurat function “DataTransfer” and the R package ComplexHeatMap (ver 2.12.1). GRC gene module scores were performed using UCell (version 2.0.1; Andreatta and Carmona, 2021). Label transfer and module score significance testing was applied using Welch two sample t-tests, and effect sizes were calculated by \log_2 fold-change. ssGSEA analysis was performed using the escape R package (version 1.6.0; Borchering et al., 2021), which utilizes the Molecular Signatures Database 3.0 (Liberzon et al., 2011).

3.9. In situ hybridization

Dual-label *in situ* hybridization was performed using previously published protocols on formaldehyde-fixed embryos. To amplify the genes of interest to be used as probes, briefly, RNA was extracted from zebra finch and chicken embryos using QIAgen RNeasy kit and transcribed into cDNA using LunaScript RT (NEB #E3010). PCR was performed using chicken or zebra finch cDNA and gene specific primers (Table S33), and Q5 hot start polymerase. PCR products were subsequently cloned into vectors using pGEM-T Easy Vector System II (Promega, Cat# A1380) according to manufacturer’s instructions. Reverse primers were designed with a T3 polymerase binding site for anti-sense transcription. RNA probes were transcribed and labeled with either FITC (fluorescein isothiocyanate) or DIG (digoxigenin) NTPs (Roche Cat#).

Zebra finch and chicken embryos from stages HH25, HH28, HH36 were collected and fixed using 4% PFA and embedded in OCT. Embryos were sectioned using Leica CM 1950 Cryostat at 11 μm thickness and preserved on Fisherbrand Superfrost Plus Microscope slides.

Dual-label fluorescent *in situ* hybridization (FISH) utilized species-specific probes according to a previous publication’s protocol (Biegler et al., 2021). Slides were counterstained using 1x DAPI, imaged using a Zeiss LSM 780 confocal microscope, and processed using ImageJ (ver

2.0.0-rc-69/1.52p) and Adobe Photoshop CC (ver 24.6.0).

4. Discussion

The study of avian germ cell biology and reproductive development has overwhelmingly focused on chicken and other poultry species, despite the incredible diversity of birds (Flores-Santin and Burggren, 2021; Jarvis et al., 2014). Using scRNAseq datasets in tandem with spatial gene expression validation by RNA *in situ* hybridization, we uncovered key differences in the gene expression, sexual dimorphism, and developmental timing of gonadal germ cells between chicken and zebra finch. Our finding that both sexes in zebra finch possess two germ cell populations in the HH28 gonad, occurring as early as HH25, offers a host of implications for understanding the evolution of developmental reproductive biology of birds.

The HH28 zebra finch zGC1 and chicken cGC cells both expressed conserved PGC markers of migration and pluripotency, such as *NANOG*, *PRDM14*, *CXCR4* and *KIT* (Magnúsdóttir et al., 2013; Okuzaki et al., 2019; Sánchez-Sánchez et al., 2010). Interestingly, zGC1 lacked significant expression of *POU5F3* and *LIN28A*, which have critical roles in chicken PGC migration and pluripotency (Meng et al., 2022; Suzuki et al., 2023). In chicken, PGC markers precipitously decreased at later developmental timepoints in male and female germ cell clusters, corresponding to a gonial cell transition (Rengaraj et al., 2022).

The zebra finch zGC2 population lacked expression of these PGC marker genes, paralleling a *FOXL2L* + cGC2 population in the HH36 female chicken gonad, when RA-mediated oogenesis is known to begin (Ayers et al., 2015; Rengaraj et al., 2022; Smith et al., 2008). This process peaks around HH40 (ED14), coinciding with a peak in *FOXL2L* expression in the chicken left ovary (Ichikawa et al., 2019). That study did not find any *FOXL2L* activation in the male gonads prior to hatching, concordant with the absence of *FOXL2L* + cells in the male chicken datasets examined in our study. Significantly, this sexual dimorphism was not seen in the zebra finch, as *FOXL2L* was present in both male and female zGC2 populations.

In medaka, a teleost fish, *FOXL2L* (previously denoted as *FOXL3*) is expressed in sexually indifferent, post-migratory gonial stem cells (Tanaka, 2016), serving as an intrinsic suppressor of spermatogenesis in male and female embryos (Nishimura et al., 2015). In female teleosts *FOXL2L* expression also initiates clonal expansion of germ cells through *REC8A*- and *FBXO47*-mediated pathways of oogenesis (Kikuchi et al., 2020; Liu et al., 2022), while in males *FOXL2L* is repressed by *DMRT1* prior to mitotic germline expansion (Dai et al., 2021; Nishimura et al., 2015). In the hermaphroditic orange grouper, *FOXL2L* is activated at the mitotic onset of spermatogenesis (Lin et al., 2020), highlighting the flexible nature of *FOXL2L*-mediated mechanisms of gametogenic initiation. As zGC2 cells possessed elevated expression of mitotic genes and a clustered morphology in the gonads, it is possible that *FOXL2L* expression in the zebra finch germline plays a similar role to teleost that activates germ cell differentiation and clonal expansion. This is a departure from developmental trajectories established in the male chicken gonad, where gonocyte expansion initiates and progresses in a *FOXL2L*-independent fashion (Ichikawa et al., 2019; Rengaraj et al., 2022; Swift, 1916). It is unclear what eventually happens to these zGC2 cells, as *FOXL2L* expression persists in both male and female zebra finch gonads by HH36. The retention of these populations suggests that either a teleost-like “masculinization” of the male germline has not yet begun by this stage, or that *FOXL2L* plays a novel role in male germline development in the zebra finch. A wider characterization of *FOXL2L* expression over additional stages of avian gonadal development may help resolve these nuances in germline sex determination, not only in the zebra finch but for other species as well.

The zebra finch GRC may also act as a driver of the dramatic differences found between chicken and zebra finch germ cell development. The programmed elimination of the zebra finch GRC during somatic specification and spermatogenesis suggests a unique role for its gene

paralogs, potentially to avoid gene regulation conflicts in somatic tissues (Vontzou et al., 2023). Our study utilized available gene annotations from a partially sequenced GRC (Biederman et al., 2018; Kinsella et al., 2019), finding significant GRC gene expression differences between zGC1 and zGC2 clusters that did not mirror the expression profiles of their A chromosome counterparts. This germ cell upregulation was also not mirrored by chicken A chromosome orthologs, suggesting that these GRC gene sequences are uniquely regulated in the zebra finch to provide novel germ cell functions. In chicken, male and female PGCs do respectively differ in expression of *SMAD7* (Chr Z) or *SMAD7B* (Chr W) that provides a mechanism for sexually dimorphic developmental trajectories in germ cells (Doddamani, 2020). As the GRC is predicted to contain paralogs of genes with known roles in germline development (e.g., *PRDM1*; Magnúsdóttir et al., 2013; Kinsella et al., 2019), it is possible that this chromosome influences germline development in an asexual manner. Future work to characterize the GRC and GRC gene roles through sequencing and functional studies will be critical to identify its potential impact on songbird germline development.

Across vertebrates, germ cell development and sexual differentiation are largely dependent on extrinsic stimuli from the gonadal environment, for example by sex hormones. In the zebra finch HH28 gonad, markers of sex hormone biosynthesis (e.g., *HSD3B1*, *HSD17B1*, *CYP19A1*) were more highly expressed than in the chicken at HH28, consistent with earlier gonadal maturation and sex determination necessary for meiotic onset. This finding aligns with previous work comparing the rate of decline in *PAX2*+ IM progenitors in favor of Pre-Sertoli/Granulosa cells, denoting an accelerated maturation of somatic cells in the zebra finch gonad compared to chicken (Estermann et al., 2021). Recent work has shown that chicken PGCs are bipotent for either male or female gametogenesis depending on the somatic environment of the gonad (Ballantyne et al., 2021a, 2021b), highlighting the dominant role of extrinsic factors in chicken gamete development. Future work would be necessary to determine whether this is also true of the zebra finch or other bird species.

Interestingly, we did not observe upregulation of *STRA8* in the zGC2 population of either sex, which in the HH36 fcGC2 population corresponds with an RA-mediated onset of oogenesis (Bowles et al., 2006; Koubova et al., 2006; Smith et al., 2008). Instead, RA receptors and other markers of RA signaling (e.g., *RBP5*) were expressed in both zGC1 and zGC2 clusters, suggesting another difference in zebra finch and chicken germ cell developmental strategies. One interpretation aligns with a primed state of sexually indifferent zGC1 and zGC2 populations towards later developmental stages, though the germ cells in several teleost fish species undergo sexual differentiation independent of *STRA8*, utilizing other signals in tandem with other RA-interacting proteins, such as *Rec8a* (Adolfi et al., 2021; Crespo et al., 2019). Beyond developmental biology, our study has important implications for the long-term maintenance of zebra finch PGCs *in vitro*. In chicken, HH28 gonadal PGCs can be used to generate stable cultures (Choi et al., 2010; Han et al., 2002; Shiue et al., 2009; Szczerba et al., 2020), but it has been difficult to obtain stable PGC cultures from other bird species, regardless of the collection stage. In previous work, we successfully cultured zebra finch gonadal PGCs for several days, injected them in host embryonic gonads, and identified some host gonad reconstitution (Jung et al., 2019). This highlights the value of embryonic zebra finch gonads for gene manipulation and biobanking applications. However, these methods produce low yields of migratory-competent zebra finch PGCs and have not enabled long-term cultures. One reason for this could be due to the heterogeneity of gonadal germ cell states we found here, some having already progressed beyond a PGC state. For instance, we identified differential expression of growth factor receptor genes between chicken and zebra finch germ cell clusters, including those in the TGF-beta superfamily signaling pathway, suggesting those factors essential for chicken PGC cultures may not have a conserved role in zebra finch (Whyte et al., 2015). Our findings also predict that zebra finch PGCs may also be more sensitive to progesterone and RA,

commonly found in serum and serum replacements. The zGC1 cells also showed upregulation of many genes involved in JAK/STAT signaling. This pathway has important roles across many vertebrate stem cell lines, including in chicken spermatogonial stem cells (Herrera and Bach, 2019; Zhang et al., 2015). Recently, short-term cultures of blood-derived zebra finch PGCs have been reported (Gessara et al., 2021), adapting culture conditions used for chicken blood PGCs. As blood-derived PGCs likely represent a purer population with strong migratory cues compared to gonadal PGCs, blood PGCs may be more appropriate for derivation of long-term songbird PGC cultures for germline transmission. Growth factor and small molecule screens of signaling pathway differences between blood and gonadal PGCs, and between species, could inform the development of long-term zebra finch germline stem cell cultures.

Our studies validated some findings of Jung et al. (2021), on heterogeneity of zebra finch PGCs, as well as differences between chicken and zebra finch (Jung et al., 2023). These include the expression of *SMC1B* in zebra finch but not chicken germ cells, and of stem cell marker expression differences between zGC clusters. However, we find one of the PGC subtypes that the authors suggest are cells undergoing biological pruning; this subtype is more likely a technical artifact resulting from not removing damaged, low-quality cells with high mitochondrial DNA content (Osorio and Cai, 2020) or with low sequence depths. This is a critical issue in single cell transcriptome analyses, as not including appropriate UMI and gene count cutoffs can lead to sample artifacts and false discovery in scRNAseq datasets (Ilicic et al., 2016; Luecken and Theis, 2019; Lun, 2018). With proper barcode removal from their dataset, we resolved exactly two clusters (zGC1 and zGC2), matching what was found in our dataset.

Jung et al. (2023) highlights a potentially enhanced role for Activin signaling in zebra finch PGCs compared to chicken. Consistent with this hypothesis, our analyses show elevated expression of Activin receptors *ACVR1* and *ACVR2B* in the zGC2 cells compared to zGC1. As this pathway has many dynamic roles across germ cell development (Wijayarathna and Kretser, 2016), we instead predict that cell culture additives supporting Activin signaling in zebra finch PGCs may cause undesirable differentiation and loss of migratory competence.

Our analyses additionally benefitted from the curation of 3' UTR annotations in the chicken and zebra finch reference genomes. Several of the most utilized scRNAseq library preparations rely on 3'-biased sequencing of mRNA, necessitating adequate gene annotation of those regions to correctly identify expression levels. For instance, our detection of *FOXL2L* gene expression in the zebra finch was the result of our manual curation and extension of NCBI gene annotations, as the default annotation for the zebra finch gene was incomplete (Ichikawa et al., 2019). As more species are studied using single-cell analyses, particularly non-model organisms, utmost importance must be given to the generation of high-quality reference genomes, such as by the Vertebrate Genomes Project (Rhie et al., 2021), as well as methods to mitigate technical artifacts in cross-species comparisons.

In closing, our study identifies a very different germ cell developmental program in a songbird, suggesting a far richer diversity in avian germ cell biology than previously identified. However, with assessments of only two species it is unclear whether the zebra finch, the chicken, or both represent outliers of germline development in the avian lineage. For instance, the abridged *in ovo* development of the altricial zebra finch embryo (14 days) relative to chicken (21 days) (Hamburger and Hamilton, 1951; Murray et al., 2013), the uniquely passerine GRC, or the intensive domestication focus on egg-laying poultry (Larson and Fuller, 2014; Rubin et al., 2010) could each contribute to evolutionarily unique quirks of these species relative to other birds. Accordingly, a more comprehensive exploration of other avian clades will determine how representative these mechanisms may be across the phylogeny. Moreover, an enhanced understanding of avian germ cell biology would be particularly insightful toward the development of methods for genetic rescue in declining and endangered populations that account for more than 14% of bird species (IUCN, 2019).

Data availability

Reference genome annotation data will be submitted to public NCBI databases. scRNAseq datasets generated in this study are available through the Gene Expression Omnibus (GEO; Accession: GSE264042). Code for Seurat processing and figure generation will be deposited on GitHub (<http://github.com/Neurogenetics-Jarvis> and <https://github.com/RockefellerUniversity>). Chicken developmental gonad datasets from Estermann et al., 2020a, 2020b) are available through GEO (Accession: GSE143337). Zebra finch HH28 gonadal datasets from Jung et al. (2021) are available through GEO (Accession: GSE177478). Requests for datasets generated should be directed toward the corresponding authors (mbiegler@rockefeller.edu, ejarvis@rockefeller.edu, anna@colossal.com).

CRediT authorship contribution statement

Matthew T. Biegler: Writing – review & editing, Writing – original draft, Visualization, Validation, Software, Resources, Project administration, Methodology, Investigation, Formal analysis, Data curation, Conceptualization. **Kirubel Belay:** Writing – review & editing, Writing – original draft, Visualization, Validation, Methodology, Investigation, Formal analysis, Data curation. **Wei Wang:** Visualization, Validation, Software, Methodology, Investigation, Formal analysis, Data curation. **Christina Szialta:** Software, Methodology. **Paul Collier:** Validation, Resources, Methodology. **Ji-Dung Luo:** Software, Methodology, Investigation, Formal analysis, Data curation. **Bettina Haase:** Validation, Methodology. **Gregory L. Gedman:** Software, Methodology, Investigation, Formal analysis. **Asha V. Sidhu:** Investigation. **Elijah Harter:** Investigation. **Carlos Rivera-López:** Methodology, Investigation, Formal analysis. **Kwame Amoako-Boadu:** Investigation. **Olivier Fedrigo:** Validation, Resources, Methodology, Formal analysis, Data curation. **Hagen U. Tilgner:** Writing – review & editing, Resources. **Thomas Carroll:** Writing – review & editing, Visualization, Validation, Software, Resources, Methodology, Investigation, Formal analysis, Data curation. **Erich D. Jarvis:** Writing – review & editing, Writing – original draft, Supervision, Project administration, Funding acquisition, Formal analysis, Data curation, Conceptualization. **Anna L. Keyte:** Writing – review & editing, Writing – original draft, Visualization, Validation, Supervision, Software, Resources, Project administration, Methodology, Investigation, Funding acquisition, Formal analysis, Data curation, Conceptualization.

Declaration of generative AI and AI-assisted technologies in the writing process

During the preparation of this work, the authors used OpenAI's ChatGPT4 for early structural organization for part of the manuscript and in early proofreading for clarity. After using this service, the authors reviewed and edited the content as needed, and take full responsibility for the content of the publication.

Declaration of competing interest

The authors declare that they have no known competing financial interests or personal relationships that could have appeared to influence the work reported in this paper.

Acknowledgements

This work was done in part with assistance and equipment from Rockefeller University's Bioinformatics and Bio-Imaging Resource Centers (RRID:SCR_017791), as well as the Vertebrate Genome Laboratory. Funding for this study was provided by the Revive & Restore Biotechnology for Bird Conservation Program, the Howard Hughes Medical Institute, and the National Science Foundation (EDGE Grant

#1645199). The authors thank Alexander Suh, John Bracht, Gist Croft, Bruce Draper, Florence Marlow, Carlos Lois, Blanche Capel, Samara Brown, Graham Kelly, Owen Farchione, and Ben Novak for insightful feedback on the data and manuscript.

Appendix A. Supplementary data

Supplementary data to this article can be found online at <https://doi.org/10.1016/j.ydbio.2024.08.006>.

References

- Adolfi, M.C., Herpin, A., Martinez-Bengochea, A., Kneitz, S., Regensburger, M., Grunwald, D.J., Schartl, M., 2021. Crosstalk between retinoic acid and sex-related genes controls germ cell fate and gametogenesis in medaka. *Front. Cell Dev. Biol.* 8, 613497 <https://doi.org/10.3389/fcell.2020.613497>.
- Aleksander, S.A., Balhoff, J., Carbon, S., Cherry, J.M., Drabkin, H.J., Ebert, D., Feuermann, M., Gaudet, P., Harris, N.L., Hill, D.P., Lee, R., Mi, H., Moxon, S., Mungall, C.J., Muruganugan, A., Mushayahama, T., Sternberg, P.W., Thomas, P.D., Auken, K.V., Ramsey, J., Siegle, D.A., Chisholm, R.L., Fey, P., Aspromonte, M.C., Nuges, M.V., Quaglia, F., Tosatto, S., Giglio, M., Nadendla, S., Antonazzo, G., Attrill, H., Santos, G dos, Marygold, S., Strelets, V., Tabone, C.J., Thurmond, J., Zhou, P., Ahmed, S.H., Asanithong, P., Buitrago, D.L., Erdol, M.N., Gage, M.C., Kadhum, M.A., Li, K.Y.C., Long, M., Michalak, A., Pesala, A., Pritazahra, A., Saverimuttu, S.C.C., Su, R., Thurlow, K.E., Lovering, R.C., Logie, C., Oliferenko, S., Blake, J., Christie, K., Corbani, L., Dolan, M.E., Drabkin, H.J., Hill, D.P., Ni, L., Sitnikov, D., Smith, C., Cuzick, A., Seager, J., Cooper, L., Elser, J., Jaiswal, P., Gupta, P., Jaiswal, P., Naithani, S., Lera-Ramirez, M., Rutherford, K., Wood, V., Pons, J.L.D., Dwinell, M.R., Hayman, G.T., Kaldunski, M.L., Kwitek, A.E., Lauderkind, S.J.F., Tutaj, M.A., Vedi, M., Wang, S.-J., D'Eustachio, P., Aimo, L., Axelsen, K., Bridge, A., Hyka-Nouspikel, N., Morgat, A., Aleksander, S.A., Cherry, J.M., Engel, S.R., Karra, K., Miyasato, S.R., Nash, R.S., Skrzypek, M.S., Weng, S., Wong, E.D., Bakker, E., Berardini, T.Z., Reiser, L., Auchincloss, A., Axelsen, K., Argoud-Puy, G., Blatter, M.-C., Boutet, E., Breuza, L., Bridge, A., Casals-Casas, C., Coudert, E., Estreicher, A., Famiglietti, M.L., Feuermann, M., Gos, A., Gruaz-Gumowski, N., Hulo, C., Hyka-Nouspikel, N., Jungo, F., Mercier, P.L., Lieberherr, D., Masson, P., Morgat, A., Pedrucci, I., Pourcel, L., Poux, S., Rivoire, C., Sundaram, S., Bateman, A., Bowler-Barnett, E., Bye-A-Jee, H., Denny, P., Ignatchenko, A., Ishtiaq, R., Lock, A., Lussi, Y., Magrane, M., Martin, M.J., Orchard, S., Raposo, P., Speretta, E., Tyagi, N., Warner, K., Zaru, R., Diehl, A.D., Lee, R., Chan, J., Diamantakis, S., Raciti, D., Zarowiecki, M., Fisher, M., James-Zorn, C., Ponferrada, V., Zorn, A., Ramachandran, S., Ruzicka, L., Westerfield, M., Aleksander, S.A., Balhoff, J., Carbon, S., Cherry, J.M., Drabkin, H.J., Ebert, D., Feuermann, M., Gaudet, P., Harris, N.L., Hill, D.P., Lee, R., Mi, H., Moxon, S., Mungall, C.J., Muruganugan, A., Mushayahama, T., Sternberg, P.W., Thomas, P.D., Auken, K.V., Ramsey, J., Siegle, D.A., Chisholm, R.L., Fey, P., Aspromonte, M.C., Nuges, M.V., Quaglia, F., Tosatto, S., Giglio, M., Nadendla, S., Antonazzo, G., Attrill, H., Santos, G dos, Marygold, S., Strelets, V., Tabone, C.J., Thurmond, J., Zhou, P., Ahmed, S.H., Asanithong, P., Buitrago, D.L., Erdol, M.N., Gage, M.C., Kadhum, M.A., Li, K.Y.C., Long, M., Michalak, A., Pesala, A., Pritazahra, A., Saverimuttu, S.C.C., Su, R., Thurlow, K.E., Lovering, R.C., Logie, C., Oliferenko, S., Blake, J., Christie, K., Corbani, L., Dolan, M.E., Drabkin, H.J., Hill, D.P., Ni, L., Sitnikov, D., Smith, C., Cuzick, A., Seager, J., Cooper, L., Elser, J., Jaiswal, P., Gupta, P., Jaiswal, P., Naithani, S., Lera-Ramirez, M., Rutherford, K., Wood, V., Pons, J.L.D., Dwinell, M.R., Hayman, G.T., Kaldunski, M.L., Kwitek, A.E., Lauderkind, S.J.F., Tutaj, M.A., Vedi, M., Wang, S.-J., D'Eustachio, P., Aimo, L., Axelsen, K., Bridge, A., Hyka-Nouspikel, N., Morgat, A., Aleksander, S.A., Cherry, J.M., Engel, S.R., Karra, K., Miyasato, S.R., Nash, R.S., Skrzypek, M.S., Weng, S., Wong, E.D., Bakker, E., Berardini, T.Z., Reiser, L., Auchincloss, A., Axelsen, K., Argoud-Puy, G., Blatter, M.-C., Boutet, E., Breuza, L., Bridge, A., Casals-Casas, C., Coudert, E., Estreicher, A., Famiglietti, M.L., Feuermann, M., Gos, A., Gruaz-Gumowski, N., Hulo, C., Hyka-Nouspikel, N., Jungo, F., Mercier, P.L., Lieberherr, D., Masson, P., Morgat, A., Pedrucci, I., Pourcel, L., Poux, S., Rivoire, C., Sundaram, S., Bateman, A., Bowler-Barnett, E., Bye-A-Jee, H., Denny, P., Ignatchenko, A., Ishtiaq, R., Lock, A., Lussi, Y., Magrane, M., Martin, M.J., Orchard, S., Raposo, P., Speretta, E., Tyagi, N., Warner, K., Zaru, R., Diehl, A.D., Lee, R., Chan, J., Diamantakis, S., Raciti, D., Zarowiecki, M., Fisher, M., James-Zorn, C., Ponferrada, V., Zorn, A., Ramachandran, S., Ruzicka, L., Westerfield, M., 2023. The gene Ontology knowledgebase in 2023. *Genetics* 224, iyad031. <https://doi.org/10.1093/genetics/iyad031>.
- Andreatta, M., Carmona, S.J., 2021. UCell: robust and scalable single-cell gene signature scoring. *Comput. Struct. Biotechnol. J.* 19, 3796–3798. <https://doi.org/10.1016/j.csbj.2021.06.043>.
- Aras, S., Bai, M., Lee, I., Springett, R., Hüttemann, M., Grossman, L.I., 2015. MNRR1 (formerly CHCHD2) is a bi-organellar regulator of mitochondrial metabolism. *Mitochondrion* 20, 43–51. <https://doi.org/10.1016/j.mito.2014.10.003>.
- Ayers, K.L., Lambeth, L.S., Davidson, N.M., Sinclair, A.H., Oshlack, A., Smith, C.A., 2015. Identification of candidate gonadal sex differentiation genes in the chicken embryo using RNA-seq. *BMC Genom.* 16, 704. <https://doi.org/10.1186/s12864-015-1886-5>.
- Ayers, K.L., Smith, C.A., Lambeth, L.S., 2013. The molecular genetics of avian sex determination and its manipulation. *Genesis* 51, 325–336. <https://doi.org/10.1002/dvg.22382>.

- Ballantyne, M., Taylor, L., Hu, T., Meunier, D., Nandi, S., Sherman, A., Flack, B., Henshall, J.M., Hawken, R.J., McGrew, M.J., 2021a. Avian primordial germ cells are bipotent for male or female gametogenesis. *Front. Cell Dev. Biol.* 9, 726827 <https://doi.org/10.3389/fcell.2021.726827>.
- Ballantyne, M., Woodcock, M., Doddamani, D., Hu, T., Taylor, L., Hawken, R.J., McGrew, M.J., 2021b. Direct allele introgression into pure chicken breeds using Sire Dam Surrogate (SDS) mating. *Nat. Commun.* 12, 659. <https://doi.org/10.1038/s41467-020-20812-x>.
- Bertho, S., Pasquier, J., Pan, Q., Trionnaire, G.L., Bobe, J., Postlethwait, J.H., Pailhoux, E., Schartl, M., Herpin, A., Guiguen, Y., 2016. Foxl2 and its relatives are evolutionary conserved players in gonadal sex differentiation. *Sex. Dev.* 10, 111–129. <https://doi.org/10.1159/000447611>.
- Biederman, M.K., Nelson, M.M., Asalone, K.C., Pedersen, A.L., Saldanha, C.J., Bracht, J.R., 2018. Discovery of the first germline-restricted gene by subtractive transcriptomic analysis in the zebra finch, *Taeniopygia guttata*. *Curr. Biol.* : CB 28, 1620–1627.e5. <https://doi.org/10.1016/j.cub.2018.03.067>.
- Biegler, M.T., Cantin, L.J., Scarano, D.L., Jarvis, E.D., 2021. Controlling for activity-dependent genes and behavioral states is critical for determining brain relationships within and across species. *J. Comp. Neurol.* 529, 3206–3221. <https://doi.org/10.1002/cne.25157>.
- Borcharding, N., Vishwakarma, A., Voigt, A.P., Bellizzi, A., Kaplan, J., Nepple, K., Salem, A.K., Jenkins, R.W., Zakharia, Y., Zhang, W., 2021. Mapping the immune environment in clear cell renal carcinoma by single-cell genomics. *Commun. Biol.* 4, 122. <https://doi.org/10.1038/s42003-020-01625-6>.
- Borodin, P., Chen, A., Forstmeier, W., Fouché, S., Malinovskaya, L., Pei, Y., Reifová, R., Ruiz-Ruano, F.J., Schlebusch, S.A., Sotelo-Muñoz, M., Torgasheva, A., Vontzou, N., Suh, A., 2022. Mendelian nightmares: the germline-restricted chromosome of songbirds. *Chromosome Res.* 1–18. <https://doi.org/10.1007/s10577-022-09688-3>.
- Bowles, J., Knight, D., Smith, C., Wilhelm, D., Richman, J., Mamiya, S., Yashiro, K., Chawengsaksophak, K., Wilson, M.J., Rossant, J., Hamada, H., Koopman, P., 2006. Retinoid signaling determines germ cell fate in mice. *Science* 312, 596–600. <https://doi.org/10.1126/science.1125691>.
- Buageaw, A., Sukhwani, M., Ben-Yehudah, A., Ehmcke, J., Rawe, V.Y., Pholpramool, C., Orwig, K.E., Schlatt, S., 2005. GDNF family receptor alpha1 phenotype of spermatogonial stem cells in immature mouse Testes1. *Biol. Reprod.* 73, 1011–1016. <https://doi.org/10.1095/biolreprod.105.043810>.
- Cantú, A.V., Laird, D.J., 2017. A pilgrim's progress: seeking meaning in primordial germ cell migration. *Stem Cell Res.* 24, 181–187. <https://doi.org/10.1016/j.scr.2017.07.017>.
- Chambers, I., Silva, J., Colby, D., Nichols, J., Nijmeijer, B., Robertson, M., Vrana, J., Jones, K., Grotewold, L., Smith, A., 2007. Nanog safeguards pluripotency and mediates germline development. *Nature* 450, 1230–1234. <https://doi.org/10.1038/nature06403>.
- Chen, Y.-C., Lin, S.-P., Chang, Y.-Y., Chang, W.-P., Wei, L.-Y., Liu, H.-C., Huang, J.-F., Pain, B., Wu, S.-C., 2019. In vitro culture and characterization of duck primordial germ cells. *Poultry Sci.* 98, 1820–1832. <https://doi.org/10.3382/ps/pey515>.
- Choi, J.W., Kim, S., Kim, T.M., Kim, Y.M., Seo, H.W., Park, T.S., Jeong, J.-W., Song, G., Han, J.Y., 2010. Basic fibroblast growth factor activates MEK/ERK cell signaling pathway and stimulates the proliferation of chicken primordial germ cells. *PLoS One* 5, e12968. <https://doi.org/10.1371/journal.pone.0012968>.
- Clinton, M., Zhao, D., 2023. Avian sex determination: a chicken egg conundrum. *Sex. Dev.* <https://doi.org/10.1159/000529754>.
- Crespo, D., Assis, L.H.C., van de Kant, H.J.G., de Waard, S., Safian, D., Lemos, M.S., Bogerd, J., Schulz, R.W., 2019. Endocrine and local signaling interact to regulate spermatogenesis in zebrafish: follicle-stimulating hormone, retinoic acid and androgens. *Development* 146, dev178665. <https://doi.org/10.1242/dev.178665>.
- Dai, S., Qi, S., Wei, X., Liu, X., Li, Y., Zhou, X., Xiao, H., Lu, B., Wang, D., Li, M., 2021. Germline sexual fate is determined by the antagonistic action of dmrt1 and foxl3/foxl2 in tilapia. *Development* 148, 199380. <https://doi.org/10.1242/dev.199380>.
- Doddamani, D., 2020. Transcriptome Analysis of Primordial Germ Cells of Birds. Royal (Dick) School of Veterinary Studies.
- Ericson, P.G.P., Irestedt, M., Johansson, U.S., 2003. Evolution, biogeography, and patterns of diversification in passerine birds. *J. Avian Biol.* 34, 3–15. <https://doi.org/10.1034/j.1600-048x.2003.03121.x>.
- Estermann, M.A., Major, A.T., Smith, C.A., 2020a. Gonadal sex differentiation: supporting versus steroidogenic cell lineage specification in mammals and birds. *Front. Cell Dev. Biol.* 8, 616387 <https://doi.org/10.3389/fcell.2020.616387>.
- Estermann, M.A., Mariette, M.M., Moreau, J.L.M., Combes, A.N., Smith, C.A., 2021. PAX2+ mesenchymal origin of gonadal supporting cells is conserved in birds. *Front. Cell Dev. Biol.* 9, 735203 <https://doi.org/10.3389/fcell.2021.735203>.
- Estermann, M.A., Williams, S., Hirst, C.E., Roly, Z.Y., Serralbo, O., Adhikari, D., Powell, D., Major, A.T., Smith, C.A., 2020b. Insights into gonadal sex differentiation provided by single-cell transcriptomics in the chicken embryo. *Cell Rep.* 31, 107491 <https://doi.org/10.1016/j.celrep.2020.03.055>.
- Flores-Santín, J., Burggren, W.W., 2021. Beyond the chicken: alternative avian models for developmental physiological research. *Front. Physiol.* 12, 712633 <https://doi.org/10.3389/fphys.2021.712633>.
- Fujimoto, T., Ukeshima, A., Miyayama, Y., Horio, F., Ninomiya, E., 1979. Observations of primordial germ cells in the turtle embryo (*Caretta caretta*): light and electron microscopic studies. *Dev. Growth Differ.* 21, 3–10. <https://doi.org/10.1111/j.1440-169x.1979.00003.x>.
- Gessara, I., Ditttrich, F., Hertel, M., Hildebrand, S., Pfeifer, A., Frankl-Vilches, C., McGrew, M., Gahr, M., 2021. Highly efficient genome modification of cultured primordial germ cells with lentiviral vectors to generate transgenic songbirds. *Stem Cell Rep.* <https://doi.org/10.1016/j.stemcr.2021.02.015>.
- Griffiths, R., Double, M.C., Orr, K., Dawson, R.J.G., 1998. A DNA test to sex most birds. *Mol. Ecol.* 7, 1071–1075. <https://doi.org/10.1046/j.1365-294x.1998.00389.x>.
- Hafemeister, C., Satija, R., 2019. Normalization and variance stabilization of single-cell RNA-seq data using regularized negative binomial regression. *Genome Biol.* 20 <https://doi.org/10.1186/s13059-019-1874-1>, 296–15.
- Hamburger, V., Hamilton, H.L., 1951. A series of normal stages in the development of the chick embryo. *J. Morphol.* 88, 49–92. <https://doi.org/10.1002/jmor.1050880104>.
- Han, J.Y., Park, T.S., Hong, Y.H., Jeong, D.K., Kim, J.N., Kim, K.D., Lim, J.M., 2002. Production of germline chimeras by transfer of chicken gonadal primordial germ cells maintained in vitro for an extended period. *Theriogenology* 58, 1531–1539. [https://doi.org/10.1016/s0093-691x\(02\)01061-0](https://doi.org/10.1016/s0093-691x(02)01061-0).
- Herrera, S.C., Bach, E.A., 2019. JAK/STAT signaling in stem cells and regeneration: from Drosophila to vertebrates. *Development* 146, dev167643. <https://doi.org/10.1242/dev.167643>.
- Huerta-Cepas, J., Szklarczyk, D., Heller, D., Hernández-Plaza, A., Forslund, S.K., Cook, H., Mende, D.R., Letunic, I., Rattai, T., Jensen, L.J., von Mering, C., Bork, P., 2018. eggNOG 5.0: a hierarchical, functionally and phylogenetically annotated orthology resource based on 5090 organisms and 2502 viruses. *Nucleic Acids Res.* 47, gky1085 <https://doi.org/10.1093/nar/gky1085>.
- Ichikawa, K., Ezaki, R., Furusawa, S., Horiuchi, H., 2019. Comparison of sex determination mechanism of germ cells between birds and fish: cloning and expression analyses of chicken forkhead box L3-like gene. *Dev. Dynam.* 248, 826–836. <https://doi.org/10.1002/dvdy.67>.
- Ichikawa, K., Horiuchi, H., 2023. Fate decisions of chicken primordial germ cells (PGCs): development, integrity, sex determination, and self-renewal mechanisms. *Genes-basel* 14, 612. <https://doi.org/10.3390/genes14030612>.
- Ilicic, T., Kim, J.K., Kolodziejczyk, A.A., Bagger, F.O., McCarthy, D.J., Marioni, J.C., Teichmann, S.A., 2016. Classification of low quality cells from single-cell RNA-seq data. *Genome Biol.* 17, 29. <https://doi.org/10.1186/s13059-016-0888-1>.
- Imus, N., Roe, M., Charter, S., Durrant, B., Jensen, T., 2014. Transfer and detection of freshly isolated or cultured chicken (*Gallus gallus*) and exotic species' embryonic gonadal germ stem cells in host embryos. *Zool. Sci.* 31, 360–368. <https://doi.org/10.2108/zs130210>.
- IUCN, 2019. The IUCN red list of threatened species. <https://www.iucnredlist.org/resourceres/grid>.
- Jarvis, E.D., Mirarab, S., Aberer, A.J., Li, B., Houde, P., Li, C., Ho, S.Y.W., Faircloth, B.C., Nabholz, B., Howard, J.T., Suh, A., Weber, C.C., Fonseca, R.R. da, Li, J., Zhang, F., Li, H., Zhou, L., Narula, N., Liu, L., Ganapathy, G., Boussau, B., Bayzid, M.S., Zavidovych, V., Subramanian, S., Gabaldón, T., Capella-Gutiérrez, S., Huerta-Cepas, J., Rekepalli, B., Munch, K., Schierup, M., Lindow, B., Warren, W.C., Ray, D., Green, R.E., Bruford, M.W., Zhan, X., Dixon, A., Li, S., Li, N., Huang, Y., Derryberry, E.P., Bertelsen, M.F., Sheldon, F.H., Brumfield, R.T., Mello, C.V., Lovell, P.V., Wirthlin, M., Schneider, M.P.C., Prosdocimi, F., Samaniego, J.A., Velazquez, A.M.V., Alfaro-Núñez, A., Campos, P.F., Petersen, B., Sichert-Ponten, T., Pas, A., Bailey, T., Scofield, P., Bunce, M., Lambert, D.M., Zhou, Q., Perelman, P., Driskell, A.C., Shapiro, B., Xiong, Z., Zeng, Y., Liu, S., Li, Z., Liu, B., Wu, K., Xiao, J., Yinqi, X., Zheng, Q., Zhang, Y., Yang, H., Wang, J., Smeds, L., Rheindt, F.E., Braun, M., Fjelds, J., Orlando, L., Barker, F.K., Jönsson, K.A., Johnson, W., Koepfli, K.-P., O'Brien, S., Haussler, D., Ryder, O.A., Rahbek, C., Willerslev, E., Graves, G.R., Glenn, T.C., McCormack, J., Burt, D., Ellegren, H., Alström, P., Edwards, S.V., Stamatidakis, A., Mindell, D.P., Cracraft, J., Braun, E.L., Warnow, T., Jun, W., Gilbert, M.T.P., Zhang, G., 2014. Whole-genome analyses resolve early branches in the tree of life of modern birds. *Science* 346, 1320–1331. <https://doi.org/10.1126/science.1253451>.
- Jean, C., Oliveira, N.M.M., Intarapat, S., Fuet, A., Mazoyer, C., Almeida, I.D., Trevers, K., Boast, S., Aubel, P., Bertocchini, F., Stern, C.D., Pain, B., 2015. Transcriptome analysis of chicken ES, blastodermal and germ cells reveals that chick ES cells are equivalent to mouse ES cells rather than EpiSC. *Stem Cell Res.* 14, 54–67. <https://doi.org/10.1016/j.scr.2014.11.005>.
- Jung, K.M., Kim, Y.M., Keyte, A.L., Biegler, M.T., Rengaraj, D., Lee, H.J., Mello, C.V., Velho, T.A.F., Fedrigo, O., Haase, B., Jarvis, E.D., Han, J.Y., 2019. Identification and characterization of primordial germ cells in a vocal learning Neoveaves species, the zebra finch. *Faseb. J.* 33, 13825–13836. <https://doi.org/10.1096/fj.201900760rr>.
- Jung, K.M., Seo, M., Han, J.Y., 2023. Comparative single-cell transcriptomic analysis reveals differences in signaling pathways in gonadal primordial germ cells between chicken (*Gallus gallus*) and zebra finch (*Taeniopygia guttata*). *Faseb. J.* 37, e22706 <https://doi.org/10.1096/fj.202201569r>.
- Jung, K.M., Seo, M., Kim, Y.M., Kim, J.L., Han, J.Y., 2021. Single-cell RNA sequencing revealed the heterogeneity of gonadal primordial germ cells in zebra finch (*Taeniopygia guttata*). *Front. Cell Dev. Biol.* 9, 791335 <https://doi.org/10.3389/fcell.2021.791335>.
- Kim, J.N., Park, T.S., Park, S.H., Park, K.J., Kim, T.M., Lee, S.K., Lim, J.M., Han, J.Y., 2010. Migration and proliferation of intact and genetically modified primordial germ cells and the generation of a transgenic Chicken1. *Biol. Reprod.* 82, 257–262. <https://doi.org/10.1095/biolreprod.109.079723>.
- Kim, Y.-K., Cho, B., Cook, D.P., Trcka, D., Wrana, J.L., Ramalho-Santos, M., 2023. Absolute scaling of single-cell transcriptomes identifies pervasive hypertranscription in adult stem and progenitor cells. *Cell Rep.* 42, 111978 <https://doi.org/10.1016/j.celrep.2022.111978>.
- Kikuchi, M., Nishimura, T., Ishishita, S., Matsuda, Y., Tanaka, M., 2020. foxl3, a sexual switch in germ cells, initiates two independent molecular pathways for commitment to oogenesis in medaka. *Proc. Natl. Acad. Sci. USA* 117, 12174–12181. <https://doi.org/10.1073/pnas.1918556117>.
- Kinsella, C.M., Ruiz-Ruano, F.J., Dion-Côté, A.-M., Charles, A.J., Gossmann, T.I., Cabrero, J., Kappel, D., Hemmings, N., Simons, M.J.P., Camacho, J.P.M., Forstmeier, W., Suh, A., 2019. Programmed DNA elimination of germline

- development genes in songbirds. *Nat. Commun.* 10 <https://doi.org/10.1038/s41467-019-13427-4>, 5468–10.
- Koubouva, J., Menke, D.B., Zhou, Q., Capel, B., Griswold, M.D., Page, D.C., 2006. Retinoic acid regulates sex-specific timing of meiotic initiation in mice. *Proc. Natl. Acad. Sci. USA* 103, 2474–2479. <https://doi.org/10.1073/pnas.0510813103>.
- Larson, G., Fuller, D.Q., 2014. The evolution of animal domestication. *Annu. Rev. Ecol. Evol. Syst.* 45, 1–22. <https://doi.org/10.1146/annurev-ecolsys-110512-135813>.
- Lee, J.H., Park, J.-W., Kim, S.W., Park, J., Park, T.S., 2017. C-X-C chemokine receptor type 4 (CXCR4) is a key receptor for chicken primordial germ cell migration. *J. Reprod. Dev.* 63, 555–562. <https://doi.org/10.1262/jrd.2017-067>.
- Liao, Y., Smyth, G.K., Shi, W., 2019. The R package Rsubread is easier, faster, cheaper and better for alignment and quantification of RNA sequencing reads. *Nucleic Acids Res.* 47, e47. <https://doi.org/10.1093/nar/gkz114> e47.
- Liberzon, A., Subramanian, A., Pinchback, R., Thorvaldsdóttir, H., Tamayo, P., Mesirov, J.P., 2011. Molecular signatures database (MSigDB) 3.0. *Bioinformatics* 27, 1739–1740. <https://doi.org/10.1093/bioinformatics/btr260>.
- Lin, F., Tong, F., He, Q., Xiao, S., Liu, X., Yang, H., Guo, Y., Wang, Q., Zhao, H., 2020. In vitro effects of androgen on testicular development by the AR-foxl3-rec8/fbxo47 axis in orange-spotted grouper (*Epinephelus coioides*). *Gen. Comp. Endocr.* 292, 113435. <https://doi.org/10.1016/j.ygcen.2020.113435>.
- Liu, Y., Kossack, M.E., McPaul, M.E., Christensen, L.N., Siebert, S., Wyatt, S.R., Kamei, C. N., Horst, S., Arroyo, N., Drummond, I.A., Juliano, C.E., Draper, B.W., 2022. Single-cell transcriptome reveals insights into the development and function of the zebrafish ovary. *Elife* 11, e76014. <https://doi.org/10.7554/elifesciences.76014>.
- Luecken, M.D., Theis, F.J., 2019. Current best practices in single-cell RNA-seq analysis: a tutorial. *Mol. Syst. Biol.* 15, e8746. <https://doi.org/10.15252/msb.20188746>.
- Lun, A., 2018. Overcoming systematic errors caused by log-transformation of normalized single-cell RNA sequencing data. *bioRxiv* 404962. <https://doi.org/10.1101/404962>.
- Lyall, J., Irvine, R.M., Sherman, A., McKinley, T.J., Núñez, A., Purdie, A., Outtrim, L., Brown, I.H., Rolleston-Smith, G., Sang, H., Tiley, L., 2011. Suppression of avian influenza transmission in genetically modified chickens. *Science* 331, 223–226. <https://doi.org/10.1126/science.1198020>.
- Magnúsdóttir, E., Dietmann, S., Murakami, K., Günesdogan, U., Tang, F., Bao, S., Diamanti, E., Lao, K., Gottgens, B., Surani, M.A., 2013. A tripartite transcription factor network regulates primordial germ cell specification in mice. *Nat. Cell Biol.* 15, 905–915. <https://doi.org/10.1038/ncb2798>.
- Meng, L., Wang, S., Jiang, H., Hua, Y., Yin, B., Huang, X., Man, Q., Wang, H., Zhu, G., 2022. Oct4 dependent chromatin activation is required for chicken primordial germ cell migration. *Stem Cell Rev Rep* 1–12. <https://doi.org/10.1007/s12015-022-10371-7>.
- Motono, M., Ohashi, T., Nishijima, K., Iijima, S., 2008. Analysis of chicken primordial germ cells. *Cytotechnology* 57, 199–205. <https://doi.org/10.1007/s10616-008-9156-x>.
- Murray, J.R., Varian-Ramos, C.W., Welch, Z.S., Saha, M.S., 2013. Embryological staging of the zebra finch, *Taeniopygia guttata*. *J. Morphol.* 274, 1090–1110. <https://doi.org/10.1002/jmor.20165>.
- Nishimura, T., Sato, T., Yamamoto, Y., Watakabe, I., Ohkawa, Y., Suyama, M., Kobayashi, S., Tanaka, M., 2015. foxl3 is a germ cell-intrinsic factor involved in sperm-egg fate decision in medaka. *Science* 349, 328–331. <https://doi.org/10.1126/science.12657>.
- Okuzaki, Y., Kaneoka, H., Suzuki, T., Hagihara, Y., Nakayama, Y., Murakami, S., Murase, Y., Kuroiwa, A., Iijima, S., Nishijima, K., 2019. PRDM14 and BLIMP1 control the development of chicken primordial germ cells. *Dev. Biol.* 455, 32–41. <https://doi.org/10.1016/j.ydbio.2019.06.018>.
- Osorio, D., Cai, J.J., 2020. Systematic determination of the mitochondrial proportion in human and mice tissues for single-cell RNA-sequencing data quality control. *Bioinformatics* 37, 963–967. <https://doi.org/10.1093/bioinformatics/btaa751>.
- Park, T.S., Kim, M.A., Lim, J.M., Han, J.Y., 2008. Production of quail (*Coturnix japonica*) germline chimeras derived from in vitro-cultured gonadal primordial germ cells. *Mol. Reprod. Dev.* 75, 274–281. <https://doi.org/10.1002/mrd.20821>.
- Pigozzi, M.I., Solari, A.J., 1998. Germ cell restriction and regular transmission of an accessory chromosome that mimics a sex body in the zebra finch, *Taeniopygia guttata*. *Chromosome Res.* 6, 105–113. <https://doi.org/10.1023/a:1009234912307>.
- Rengaraj, D., Cha, D.G., Lee, H.J., Lee, K.Y., Choi, Y.H., Jung, K.M., Kim, Y.M., Choi, Hee Jung, Choi, Hyeon Jeong, Yoo, E., Woo, S.J., Park, J.S., Park, K.J., Kim, J.K., Han, J. Y., 2022. Dissecting chicken germ cell dynamics by combining a germ cell tracing transgenic chicken model with single-cell RNA sequencing. *Comput Struct Biotechnol J.* <https://doi.org/10.1016/j.csbj.2022.03.040>.
- Rengaraj, D., Han, J.Y., 2022. Female germ cell development in chickens and humans: the chicken oocyte enriched genes convergent and divergent with the human oocyte. *Int. J. Mol. Sci.* 23, 11412. <https://doi.org/10.3390/ijms231911412>.
- Rhie, A., McCarthy, S.A., Fedrigo, O., Damas, J., Formenti, G., Koren, S., Uliano-Silva, M., Chow, W., Fungtammasan, A., Kim, J., Lee, C., Ko, B.J., Chaisson, M., Gledhill, G.L., Cantin, L.J., Thibaud-Nissen, F., Haggerty, L., Bista, I., Smith, M., Haase, B., Mountcastle, J., Winkler, S., Paez, S., Howard, J., Vernes, S.C., Lama, T. M., Grutzner, F., Warren, W.C., Balakrishnan, C.N., Burt, D., George, J.M., Biegler, M.T., Iorns, D., Digby, A., Eason, D., Robertson, B., Edwards, T., Wilkinson, M., Turner, G., Meyer, A., Kautt, A.F., Franchini, P., Detrich, H.W., Svoldal, H., Wagner, M., Naylor, G.J.P., Pippel, M., Malinsky, M., Mooney, M., Simbirsky, M., Hannigan, B.T., Pesout, T., Houck, M., Misuraca, A., Kingan, S.B., Hall, R., Kronenberg, Z., Sović, I., Dunn, C., Ning, Z., Hastie, A., Lee, J., Selvaraj, S., Green, R.E., Putnam, N.H., Gut, I., Ghuray, J., Garrison, E., Sims, Y., Collins, J., Pelan, S., Torrance, J., Tracey, A., Wood, J., Dagnev, R.E., Guan, D., London, S.E., Clayton, D.F., Mello, C.V., Friedrich, S.R., Lovell, P.V., Osipova, E., Al-Ajli, F.O., Secomandi, S., Kim, H., Theofanopoulou, C., Hiller, M., Zhou, Y., Harris, R.S., Makova, K.D., Medvedev, P., Hoffman, J., Masterson, P., Clark, K., Martin, F.,
- Howe, Kevin, Flicek, P., Walenz, B.P., Kwak, W., Clawson, H., Diekhans, M., Nassar, L., Paten, B., Kraus, R.H.S., Crawford, A.J., Gilbert, M.T.P., Zhang, G., Venkatesh, B., Murphy, R.W., Koepfli, K.-P., Shapiro, B., Johnson, W.E., Palma, F.D., Marques-Bonet, T., Teeling, E.C., Warnow, T., Graves, J.M., Ryder, O.A., Haussler, D., O'Brien, S.J., Korch, J., Lewin, H.A., Howe, Kerstin, Myers, E.W., Durbin, R., Phillippy, A.M., Jarvis, E.D., 2021. Towards complete and error-free genome assemblies of all vertebrate species. *Nature* 592, 737–746. <https://doi.org/10.1038/s41586-021-03451-0>.
- Richardson, R.L.B.E., 2010. Mechanisms guiding primordial germ cell migration: strategies from different organisms. *Nat. Rev. Mol. Cell Biol.* 11, 37–49. <https://doi.org/10.1038/nrm2815>.
- Rubin, C.-J., Zody, M.C., Eriksson, J., Meadows, J.R.S., Sherwood, E., Webster, M.T., Jiang, L., Ingman, M., Sharpe, T., Ka, S., Hallböök, F., Besnier, F., Carlborg, Ö., Bed'hom, B., Tixier-Boichard, M., Jensen, P., Siegel, P., Lindblad-Toh, K., Andersson, L., 2010. Whole-genome resequencing reveals loci under selection during chicken domestication. *Nature* 464, 587–591. <https://doi.org/10.1038/nature08832>.
- Sánchez-Sánchez, A.V., Camp, E., Leal-Tassias, A., Atkinson, S.P., Armstrong, L., Díaz-Llopis, M., Mullor, J.L., 2010. Nanog regulates primordial germ cell migration through Cxcr4b. *Stem Cell* 28, 1457–1464. <https://doi.org/10.1002/stem.469>.
- Shiue, Y., Tailui, J., Liou, J., Lu, H., Tai, C., Shiau, J., Chen, L., 2009. Establishment of the long-term in vitro culture system for chicken primordial germ cells. *Reprod. Domest. Anim.* 44, 55–61. <https://doi.org/10.1111/j.1439-0531.2007.00990.x>.
- Smith, C.A., Roeszler, K.N., Bowles, J., Koopman, P., Sinclair, A.H., 2008. Onset of meiosis in the chicken embryo; evidence of a role for retinoic acid. *BMC Dev. Biol.* 8, 85. <https://doi.org/10.1186/1471-213x-8-85>.
- Smith, C.A., Roeszler, K.N., Ohnesorg, T., Cummins, D.M., Farlie, P.G., Doran, T.J., Sinclair, A.H., 2009. The avian Z-linked gene DMRT1 is required for male sex determination in the chicken. *Nature* 461, 267–271. <https://doi.org/10.1038/nature08298>.
- Srihawong, T., Kuwana, T., Siripattaraprat, K., Tirawattanawanich, C., 2016. Chicken primordial germ cell motility in response to stem cell factor sensing. *Int. J. Dev. Biol.* 59, 453–460. <https://doi.org/10.1387/ijdb.140287ct>.
- Stévant, I., Kühne, F., Greenfield, A., Chaboissier, M.-C., Dermitzakis, E.T., Nef, S., 2019. Dissecting cell lineage specification and sex fate determination in gonadal somatic cells using single-cell transcriptomics. *Cell Rep.* 26, 3272–3283.e3. <https://doi.org/10.1016/j.celrep.2019.02.069>.
- Stuart, T., Butler, A., Hoffman, P., Hafemeister, C., Papalexi, E., Mauck, W.M., Hao, Y., Stoeckius, M., Smibert, P., Satija, R., 2019. Comprehensive integration of single-cell data. *Cell* 177, 1888–1902.e21. <https://doi.org/10.1016/j.cell.2019.05.031>.
- Suzuki, K., Kwon, S.J., Saito, D., Atsuta, Y., 2023. LIN28 is essential for the maintenance of chicken primordial germ cells. *Cells Dev* 176, 203874. <https://doi.org/10.1016/j.cdev.2023.203874>.
- Swift, C.H., 1914. Origin and early history of the primordial germ-cells in the chick. *Am. J. Anat.* 15, 483–516. <https://doi.org/10.1002/aja.1000150404>.
- Swift, C.H., 1916. Origin of the sex-cords and definitive spermatogonia in the male chick. *Am. J. Anat.* 20, 375–410. <https://doi.org/10.1002/aja.1000200305>.
- Szczerba, A., Kuwana, T., Paradowska, M., Bednarczyk, M., 2020. In vitro culture of chicken circulating and gonadal primordial germ cells on a somatic feeder layer of avian origin. *Animals* 10, 1769. <https://doi.org/10.3390/ani10101769>.
- Tanaka, M., 2016. Germline stem cells are critical for sexual fate decision of germ cells. *Bioessays* 38, 1227–1233. <https://doi.org/10.1002/bies.201600045>.
- Tang, D., Kang, R., Livesey, K.M., Kroemer, G., Billiar, T.R., Van Houten, B., Zeh, H.J., Lotze, M.T., 2011. High-mobility group box 1 is essential for mitochondrial quality control. *Cell Metabol.* 13, 701–711. <https://doi.org/10.1016/j.cmet.2011.04.008>.
- Torgasheva, A.A., Malinovsky, L.P., Zadesnais, K.S., Karamysheva, T.V., Kizilova, E. A., Akberdin, A.A., Pristayzhnyuk, I.E., Shnaider, E.P., Volodkina, V.A., Saifitdinova, A.F., Galkina, S.A., Larkin, D.M., Rubtsov, N.B., Borodin, P.M., 2019. Germline-restricted chromosome (GRC) is widespread among songbirds. *Proc. Natl. Acad. Sci. USA* 116, 11845–11850. <https://doi.org/10.1073/pnas.1817373116>.
- van de Lavoie, M.-C., Diamond, J.H., Leighton, P.A., Mather-Love, C., Heyer, B.S., Bradshaw, R., Kerchner, A., Hooi, L.T., Gessaro, T.M., Swanberg, S.E., Delany, M.E., Etches, R.J., 2006. Germline transmission of genetically modified primordial germ cells. *Nature* 441, 766–769. <https://doi.org/10.1038/nature04831>.
- Vontzou, N., Pei, Y., Mueller, J.C., Reifová, R., Ruiz-Ruano, F.J., Schlegel, S.A., Suh, A., 2023. Songbird germline-restricted chromosome as a potential arena of genetic conflicts. *Curr. Opin. Genet. Dev.* 83, 102113. <https://doi.org/10.1016/j.gde.2023.102113>.
- Wernery, U., Liu, C., Baskar, V., Guerinche, Z., Khazanehdari, K.A., Saleem, S., Kinne, J., Wernery, R., Griffin, D.K., Chang, I.-K., 2010. Primordial germ cell-mediated chimera technology produces viable pure-line houbara bustard offspring: potential for repopulating an endangered species. *PLoS One* 5, e15824. <https://doi.org/10.1371/journal.pone.0015824>.
- Whyte, J., Glover, J.D., Woodcock, M., Brzeszczynska, J., Taylor, L., Sherman, A., Kaiser, P., McGrew, M.J., 2015. FGF, insulin, and SMAD signaling cooperate for avian primordial germ cell self-renewal. *Stem Cell Rep.* 5, 1171–1182. <https://doi.org/10.1016/j.stemcr.2015.10.008>.
- Wijayarathna, R., Kretser, D.M., 2016. Activins in reproductive biology and beyond. *Hum. Reprod. Update* 22, 342–357. <https://doi.org/10.1093/humupd/dmv058>.
- Yakhkeshi, S., Rahimi, S., Sharafi, M., Hassani, S.-N., Taleahmad, S., Shahverdi, A., Baharvand, H., 2017. In vitro improvement of quail primordial germ cell expansion through activation of TGF-beta signaling pathway. *J. Cell. Biochem.* <https://doi.org/10.1002/jcb.26618>.

Yao, C.-H., Wang, R., Wang, Y., Kung, C.-P., Weber, J.D., Patti, G.J., 2019. Mitochondrial fusion supports increased oxidative phosphorylation during cell proliferation. *Elife* 8, e41351. <https://doi.org/10.7554/elife.41351>.

Young, M.D., Behjati, S., 2020. SoupX removes ambient RNA contamination from droplet-based single-cell RNA sequencing data. *GigaScience* 9, giaa151. <https://doi.org/10.1093/gigascience/giaa151>.

Zhang, L., Zuo, Q., Li, D., Lian, C., Ahmed, K.E., Tang, B., Song, J., Zhang, Y., Li, B., 2015. Study on the role of JAK/STAT signaling pathway during chicken spermatogonial stem cells generation based on RNA-Seq. *J. Integr. Agric.* 14, 939–948. [https://doi.org/10.1016/s2095-3119\(14\)60938-2](https://doi.org/10.1016/s2095-3119(14)60938-2).